NASA
Technical
Paper
2358

November 1984

Analysis of Noise Measured From a Propeller in a Wake

P. J. W. Block

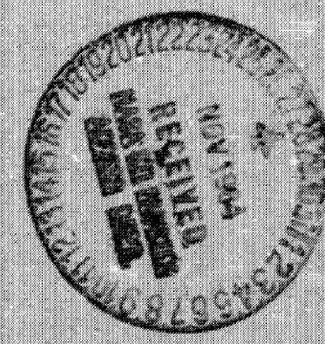

NASA

NASA Technical Paper 2358

1984

Analysis of Noise Measured From a Propeller in a Wake

P. J. W. Block

Langley Research Center
Hampton, Virginia

National Aeronautics and Space Administration

Scientific and Technical Information Branch

CONTENTS

SUMMARY

In this experimental study the acoustic characteristics of a propeller operating in a wake were studied. The propeller performance and noise were measured from two 0.25-scale propellers operating in an open jet anechoic flow environment with and without a wake. One propeller had NACA 16-series sections; the other, ARA-D. Wake thicknesses of 1 and 3 propeller chords were generated by an airfoil which spanned the full diameter of the propeller. The airfoil wake profiles were measured. Noise measurements were made at six locations in the flow, in the relative near field of the propeller at three streamwise and two azimuthal positions, and outside the flow at three streamwise positions. The propellers were operated at 40, 83, and 100 lbf (178, 369, and 445 N) of thrust. The acoustic data are analyzed, and the effects on the overall sound pressure level (OASPL) and scaled A-weighted sound level L_A with propeller thrust, wake thickness, and observer location are presented.

Analysis of the data showed that, generally, the wake increased the overall noise (OASPL) produced by the propeller; increased the harmonic content of the noise, thus the scaled L_A; and produced an azimuthal dependence. The ΔOASPL decreased with increasing propeller thrust. The OASPL increased as the wake thickness increased but the major part of the increase was observed between thickness-chord ratios (t/c) of 0 and 1. Little additional noise increase resulted between $t/c = 1$ and $t/c = 3$. The highest values of ΔOASPL were found at observer locations corresponding to 25° from the plane of the wake ($\phi = 25°$) and out of the plane of the propeller disk ($\theta = \pm 30°$). The maximum value of ΔOASPL was about 10 dB. The lowest values of ΔOASPL were observed in the disk plane and normal to the plane of the wake. The maximum value of ΔL_A was 25 dBA. This large increase reflects the large change in the frequency content of the acoustic signal when the wake is introduced. Both propellers generally produced the same trends in ΔOASPL and ΔL_A with thrust and wake thickness.

INTRODUCTION

As more economical and energy efficient air transportation is sought, propellers become a prime candidate for the propulsion of large transports (ref. 1). Among the many options for integrating these propellers onto the airframe, a "pusher" installation has been shown to have many advantages stemming from cost, weight, or aerodynamic considerations. Aerodynamically, a propeller mounted behind a wing or tail surface allows smoother, less disturbed airflow over these surfaces, which is expected to reduce the aircraft drag. Placing the propeller behind the tail surface is expected to have advantages from the interior noise standpoint as well since the propeller plane is located relatively far from the passengers.

Unfortunately, little data are available on the noise produced by a propeller operating in a wake. Although many wind-tunnel studies have been conducted on pusher propeller configurations, none were found containing noise measurements with which to guide this present study. In reference 2 an experimental study in a wind tunnel of the noise produced by a model scale propeller in a wake is described. The author points out that the data were seriously affected by floor reflections and that although a large degree of irrepeatability was encountered, "an increase of the OASPL was obvious as the wing was moved quite close to the propeller." One full-scale

flight test containing noise measurements of a pusher/tractor aircraft is reported in reference 3. The data indicated that the pusher operation was noisier than the tractor operation but the data set was limited and insufficient to determine the characteristics of the noise. These data are needed for developing and/or validating methods by which the noise impact of pusher propellers can be assessed. This present paper addresses this area with an experimental study of the noise produced by a propeller operating in an airfoil wake.

In this study, the propeller performance and noise were measured from two 0.25-scale propellers operating in an anechoic flow environment with and without a wake. One propeller had NACA 16-series sections, the other ARA-D. Wake thicknesses of one and three propeller chords were generated by an airfoil which spanned the full diameter of the propeller. The airfoil wake profiles were measured. Noise measurements were made at six locations: in the flow, in the relative near field of the propeller at three streamwise and three azimuthal positions, and outside the flow at three streamwise positions. The propellers were operated at 40, 83, and 100 lbf (178, 369, and 445 N) of thrust. All the data are presented without analysis in reference 4. A small subset of the data is contained in reference 5. In this present paper, the acoustic data are analyzed and the effects on the OASPL and scaled L_A with propeller thrust, wake thickness, and observer location are presented. Performance results are also presented for completeness.

SYMBOLS

Values are given in U.S. Customary Units with the equivalent values given parenthetically in SI Units for the convenience of the reader.

a_n, b_n, c_n	Fourier coefficients
C_P	power coefficient, $P/\rho_A n^3 d^5$
C_T	thrust coefficient, $T/\rho_A n^2 d^4$
C_p	pressure coefficient, $\frac{p - p_\infty}{q}$
c	maximum chord length of propeller blade
d	propeller diameter
d_j	jet diameter of QFF
$d_{nacelle}$	maximum diameter of PTS nacelle
J	propeller advance ratio, U/nd
L_A	A-weighted sound level
M_T	helical tip Mach number
n	number of revolutions per second

P	power absorbed by propeller
p	stagnation pressure
p_∞	free-stream static pressure
q	free-stream dynamic pressure
R	propeller radius
T	propeller thrust
T_A	air temperature
t	thickness of airfoil wake
U	tunnel velocity
x,y	Cartesian coordinates
x_1,x_2,x_3	coordinates of microphones with respect to centerline of propeller disk
α	angle of attack or pitch angle of propeller axis with respect to airstream
β	propeller pitch with respect to plane of rotation
$\beta_{.75}$	propeller blade pitch setting at 0.75R radial station
η	propeller efficiency
θ	angle of microphone with respect to propeller disk plane
ϕ	angle of microphone with respect to wake
ρ_A	air density

Abbreviations:

BPF	blade passage frequency
mic	microphone
OASPL	overall sound pressure level
ΔOASPL	OASPL with wake minus OASPL without wake (uniform flow)
SPL	sound pressure level
PTS	propeller test stand
QFF	quiet flow facility

DESCRIPTION OF EXPERIMENT

Models, Test Apparatus, and Facility

Propellers.- The two propellers used in the experiment were three-bladed, 0.25-scale model propellers designed for the same twin-engine airplane. The two designs are designated Twin 1 and Twin 3. Both propellers were 2.21 ft (0.674 m) in diameter. The chord and twist distributions and airfoil sections are given in figures 1 and 2. The two propeller designs are similar. The most notable difference is the airfoil sections employed. In particular Twin 3 has a much larger leading-edge radius. Twin 1 has Clark Y airfoil sections inboard and modified NACA 16-series sections outboard (fig. 1(b)). Twin 3 has ARA-D sections (fig. 2(b)). The different airfoil sections are expected to produce distinctly different pressure distributions over the two propeller surfaces. Both propellers were fabricated from aluminum by using three- and five-axis numerically controlled milling machines, and they were dynamically balanced. When set in their respective hubs, the propeller pitch settings were adjustable in 0.5° increments and were secured by a locking pin. The pitch angle $\beta_{.75}$ was read at the 75-percent radial position by resting an inclinometer flat against the lower surface. With this arrangement the pitch-angle readings were accurate to 0.5° and were repeatable. The propeller section data were used to determine the actual geometric angle of the chord line with respect to the plane of rotation.

Propeller test stand (PTS).- The PTS nacelle is a cylindrically shaped shell with a maximum outside diameter of 9 in. (0.229 m) and overall length of 76 in. (1.93 m). It houses a quiet 50-hp, water-cooled, variable-speed synchronous electric motor having a maximum speed of 8000 rpm. The motor turned the propellers clockwise looking upstream. The PTS was mounted coaxially with a 4-ft-diameter (1.22-m) circular jet which simulated the forward velocity for the propellers. A more complete description of the PTS and its operation in the quiet flow facility is given in reference 6.

Quiet flow facility (QFF).- The QFF, located at the Langley Research Center, is a large anechoic room with a quiet, very low turbulence flow supply. A complete description of the flow and anechoic characteristics of the QFF is given in reference 7. The maximum exit velocity of the 4-ft-diameter (1.22-m) jet is 120 fps (36.6 m/s). A schematic of the PTS in the QFF showing its location and other appropriate dimensions is given in figure 3. The nose of the spinner of the PTS was 30.25 in. (0.77 m) from the exit of the jet.

In order to avoid corrections to the propeller performance, the method described in reference 6 was employed which gives the operational limits for a propeller in an open jet. This limit is given as

$$\frac{C_T}{J^2} < \frac{\pi}{8}\left(\frac{d^2 - d_{nacelle}^2}{d^2}\right)\left\{\left[\frac{2(0.62d_j)^2}{d^2 - d_{nacelle}^2} - 1\right]^2 - 1\right\} \qquad (1)$$

This criterion gives the maximum amount of thrust that a propeller can produce at a given advance ratio which is determined by the propeller diameter (2.21 ft (0.674 m))

and the jet diameter (4 ft (1.22 m)). For these tests the operational limit for no corrections to be made to the propeller performance is

$$\frac{C_T}{J^2} < 0.837$$

Wake-producing airfoil.- To introduce a wake or velocity defect region into the propeller, an NACA 0020 airfoil was used. This airfoil was placed directly upstream of the spinner and spanned the 4-ft-diameter (1.22-m) jet. A photograph of the airfoil upstream of the propeller is shown in figure 4. The airfoil was closer to the spinner than the photograph shows, and the two airfoils behind the propeller were not used during these tests. The angle of attack of the wake-producing airfoil was manually adjustable. An angle of attack of 15° was used to produce the narrower wake which was 1 propeller chord thick ($t/c \approx 1$). At an angle of attack of 20.4°, the flow over the airfoil was fully separated, and the wake thickness was measured to be 3 propeller chords thick ($t/c \approx 3$). These wake thicknesses were chosen to provide the data necessary to validate a quasi-steady noise prediction method although no predictions are presented in this paper. The measurements of the velocity defect region produced by the airfoil are given in a later section. The dimensions and relative position of the airfoil with respect to the propeller disk are shown in figure 5. The airfoil position was shifted when its angle of attack was changed so that the center of the sheet of turbulent flow which constitutes the wake would be a diameter of the propeller disk. A secondary effect of the airfoil was to turn the flow coming into the propeller disk. No measurements were made to determine how much or how uniformly the flow was turned. For calculation purposes, the angle of the flow into the disk was assumed to be equal to the angle of attack of the airfoil.

Microphone locations.- Noise measurements were made inside and outside of the flow at the microphone locations shown in figure 6. The measurements were made in the propeller plane ($\theta = 0°$) and 30° upstream ($\theta = -30°$) and downstream ($\theta = +30°$) from the propeller plane. Microphone 3, the only microphone in the flow, was 1/4 in. (6.35 mm) in diameter and had a bullet-shaped nose. It was held in the flow by a specially designed rigid streamlined holder and by an adjustable stand. This microphone was positioned to as many as six locations for a given condition. The closest of these positions was 4.75 in. (0.121 m) or 0.18 propeller diameters from the tip of the propeller. Microphones 4, 5, and 6 were located on a fixed stand outside of the flow. These microphones were 0.5 in. (12.7 mm) in diameter and had a simple protective grid cap. The closest of these positions was the in-plane microphone (mic 5) which was 23.35 in. (0.593 m) or 0.881 propeller diameters from the tip.

When the wake-producing airfoil was installed upstream of the propeller, microphone 3 was positioned at the three streamwise locations ($\theta = -30°$, 0°, and +30°) for each of two azimuthal locations ($\phi = 25°$ and 90°). The azimuthal angle ϕ is the angle measured from the wake-producing airfoil as shown in figure 6. The fixed stand holding microphones 4, 5, and 6 was oriented $\phi = 77°$ from the plane of the airfoil. All microphone locations are given in table 1 in terms of the Cartesian coordinate system shown in figure 7 and the polar coordinate system shown in figure 6.

Test Conditions

The test consisted of the propeller performance measurements and the propeller noise measurements. The conditions for the performance measurements are given in

table 2; the conditions for the noise measurements, in table 3. All tests were conducted at a forward speed of 120 fps (36.6 m/s).

The performance measurements (table 2) were conducted over a series of rotational speeds for each blade pitch angle and in-flow condition. The x-marks in table 2 indicate conditions where a series of propeller performance measurements were made; the asterisks indicate the conditions where noise measurements were made.

The conditions for the noise measurements are expanded and given in table 3. These tests were conducted at rotational speeds corresponding to desired thrust settings. Both propellers were tested at thrust levels of 40 lbf (178 N) and 83 lbf (369 N). Twin 3 was also tested at 100 lbf (445 N). The measured values of the air temperature, propeller rotational speed (rpm), and thrust are given in table 3 along with the computed values for ρ_A, C_T, C_P, J, and M_T.

Measurements and Data Reduction

Propeller force data.- The propeller thrust was measured by a load cell located aft of the motor and grounded to the case. (See ref. 6.) The torque was measured by an in-line rotating shaft torque sensor which was isolated by two decouplers. The average rotational speed (rpm) and data from the thrust load cell and torque sensors were recorded by a computer and stored on a disk. These data were acquired beginning at a rotational speed which gave a minimum of 5 lbf (22.3 N) of thrust. The propeller thrust and torque were sampled in increments of 200 rpm until the maximum speed (8000 rpm) or motor torque (29 ft-lb (39 N-M)) was reached. The speed was then decreased in 200-rpm increments to the beginning value.

The repeatability test cases showed that the thrust and power coefficient variation was less than 0.004.

The propeller operating conditions (C_T/J^2) were evaluated to ensure that the free jet contraction (due to the propeller operation) did not require a correction to the force data. (See eq. (1).) Data requiring such a correction were purged from the data base and are not presented in this paper.

The propeller thrust and torque data are presented in terms of the thrust and power coefficients (C_T and C_P) and the efficiency (η). Normally these coefficients are plotted against the advance ratio, $J = U/nd$. In these tests, however, the airfoil introduced a flow angle of attack into the propeller disk. In these cases, the inflow velocity to the disk is $U \cos \alpha$ where α is the angle of the inflow with respect to the propeller axis. The angle of the flow into the propeller is assumed to be the geometric angle of attack of the wake-producing airfoil. Thus, the performance data are plotted against $J \cos \alpha$ instead of J, and the efficiency is calculated as

$$\eta = \frac{C_T}{C_P} J \cos \alpha$$

Wake data.- The airfoil wake was surveyed at the propeller plane to determine its position and thickness. (The propeller was not mounted on the PTS during these tests.) This survey was done with a pitot-static tube whose position was computer controlled through a stepping motor. These data had a twofold purpose. First, the wake thickness was used to determine the airfoil angle of attack that was necessary

to produce a wake which was 1 propeller chord thick (t/c = 1) and 3 propeller chords thick (t/c = 3). These angles were 15° and 20.4°, respectively. Second, the wake survey data were used to position the airfoil so that the center of the wake would intersect the propeller disk plane along a diameter.

Acoustic data.- The propeller noise data were obtained both in the flow and out of the flow at the microphone locations given previously. The acoustic data were not corrected for shear layer effects. During the test, the acoustic data and a once-per-revolution signal from the shaft were recorded at 30 in/sec (0.8 m/sec) on 1-in. magnetic tape for posttest analysis. The once-per-revolution signal was used to accurately measure the rotational speed which was an integral part of the data analysis. The analysis proceeded as follows. Each data channel was sampled at 80 000 Hz along with the once-per-revolution signal. The latter signal was used to document the period of the noise signal for each revolution of data. A harmonic analysis of each revolution yielded the Fourier coefficients a_n and b_n where n is the number of the harmonic of the blade passage frequency. The Fourier coefficients were averaged for each revolution to produce $\bar{a}_n$ and $\bar{b}_n$. From these the magnitude of the noise component at each harmonic was computed by using

$$c_n^2 = \bar{a}_n^2 + \bar{b}_n^2$$

These values were then converted to dB (re 20 μPa). This procedure was used to enhance the periodic components of the propeller noise signal while reducing the contribution of the random components via the averaging process. The random components are defined as those which are not related to the passage of the propeller blades such as the wake noise of the airfoil.

All the acoustic data are contained in reference 4. An analysis of these results is presented herein. Their presentation includes ΔOASPL, OASPL, and scaled A-weighted sound level versus propeller thrust, wake thickness, and observer location; ΔOASPL is defined as OASPL measured with the propeller operating in the wake minus OASPL measured with the propeller operating in a uniform inflow. The scaled A-weighted sound level was calculated from the harmonic analysis in two steps. First, the blade passage frequency of the propeller was scaled to full scale. For the 0.25-scale propellers employed herein, this scaling involved dividing the BPF (and its harmonics) by a factor of 4. The next step involved a simple A-weighting of the measured spectral levels according to the scaled-down frequency and summing over 20 harmonics to obtain L_A. The scaled A-level was used because it emphasizes the higher frequency components of the noise whereas OASPL emphasizes the higher levels which are usually the lower harmonics.

DISCUSSION OF RESULTS

Airfoil Wake Data

The wake survey data were normalized by the free-stream dynamic pressure. The nondimensionalized pressures for angles of attack of 15° and 20.4° are given in figure 8. It must be noted that these profiles do not take into account the suction effects of the propeller.

Propeller Performance

The thrust, power, and efficiency data pertinent to the noise tests (items with an asterisk in table 2) are presented in figures 9 and 10 for Twin 1 and Twin 3, respectively. All the data are plotted against $J \cos \alpha$ as described previously. The conditions at which the noise data were obtained are listed in table 3. The advance ratio in this table should be multiplied by $\cos \alpha$ to correspond to the abscissa in figures 9 and 10. The propeller thrust, power, and efficiency curves for all the test conditions given in table 2 are provided in reference 4.

The effect of the wake on C_T and C_P is almost negligible for both propellers; however, a small but consistent decrease in C_T and C_P can be observed when the wake is introduced. Another small but consistent decrease can be seen as the wake thickness increases. The more noticeable effect of the wake on the propeller performance is seen in the efficiency data (figs. 9(c) and 10(c)). In these figures, the highest efficiency is calculated for the propeller operating in a $t = 3c$ wake. This result is observed for both propellers although there is much data scatter near the peak efficiency.

Propeller Noise

The propeller acoustic data are presented in reference 4 and a typical result is given in figure 11. Of note is the effect of the wake on the pressure time history and the spectrum. Sharp spikes that are introduced in the time history result in an increase in all the harmonics, particularly the higher harmonics. The following discussion addresses the trends seen in the overall noise (OASPL) which is most sensitive to the change in the lower harmonics, and the scaled A-weighted sound level (L_A), which is more sensitive to the change in the higher harmonics.

Effect of propeller thrust.- In figure 12, ΔOASPL as a function of the propeller thrust for both propellers and wake thicknesses is presented. In general, ΔOASPL decreases with increasing thrust. In other words, the contribution of the sharp spikes is greatest at the lowest thrust loadings of the propellers. The slope, or rate of decrease of ΔOASPL with increasing thrust, is greater at microphone positions corresponding to 30° downstream ($\theta = +30°$) of the propeller disk plane (microphones 3c, 3f, and 6). The maximum value of ΔOASPL is about 10 dB. This maximum value was measured at the lowest thrust (40 lbf (178 N)) and at 30° downstream of the disk plane ($\theta = +30°$) and 25° to the airfoil ($\phi = 25°$) in the flow (microphone 3c). The out-of-flow microphones 4 and 6 ($\theta = \pm 30°$, $\phi = 77°$) record values between 8 and 9 dB.

For most of the cases presented in figure 12, both propellers are producing about the same magnitude of ΔOASPL and the same trends with the thrust loading. Thus, ΔOASPL does not appear to be strongly dependent on the type of propeller airfoil sections. It may be pointed out, however, that behind the propeller (30° downstream), Twin 1 consistently produces higher values of ΔOASPL than Twin 3. Understanding this behavior may depend on a knowledge of the change of surface pressure distribution as the propeller blade goes through the wake.

Effect of wake thickness.- OASPL for all the test conditions as a function of wake thickness is given in figure 13 in order of the test conditions listed in table 3. All the microphone data are presented according to location with respect to the disk plane (θ). Generally, most of the increase in OASPL due to the wake occurs in going from no wake ($t/c = 0$) to $t/c = 1$. Little additional increase is seen in

going from $t/c = 1$ to $t/c = 3$. In these figures a straight line is used to connect the symbols for ease of comparison and is not intended to imply a linear dependence on OASPL in going from zero wake thickness to $t/c = 1$. One might expect the noise level to increase sharply at the introduction of a very small wake and taper as the wake thickness approaches 1 propeller chord.

Some of the azimuthal characteristics of the noise data can also be seen in figure 13. The data presented in these figures show that the highest noise levels occur at 25° to the airfoil. The data taken at 25° and 77° to the airfoil both follow the same trends with increasing wake thickness, whereas the data at 90° to the airfoil appear to be minimally affected by the presence of the wake. As observed previously in the discussion of the effect of propeller thrust, both propellers are producing the same trends with wake thickness. This trend is seen when comparing figure 13(a) with figure 13(c) for 40 lbf (178 N) of thrust and figure 13(b) with figure 13(d) for 83 lbf (369 N) of thrust.

Dependence of ΔOASPL on position with respect to disk plane (θ).- The additional noise levels are presented as a function of θ in figure 14. The data obtained in the flow (mic 3, $\phi = 25°$ and 90°) and out of the flow (mics 4, 5, and 6, $\phi = 77°$) are given for both wake thicknesses in order of the test conditions listed in table 3. The data show that the greatest increases in ΔOASPL occur out of the plane of the propeller disk ($\theta = \pm 30°$). The least change in the noise is seen normal to the wake or airfoil ($\phi = 90°$). The changes observed at $\phi = 25°$ and 77° are typically much above that at $\phi = 90°$. Also of note is that both propellers are generating the same trends in ΔOASPL with θ.

Effect of scaled A-weighting.- In figures 12, 13, and 14, the effects of the thrust, wake thickness, and observer location on OASPL or ΔOASPL were presented, respectively. The effects of the same parameters on ΔL_A or L_A are presented in figures 15, 16, and 17. These figures parallel figures 12, 13, and 14.

Figure 15 shows the effect on ΔL_A of increasing propeller thrust. The trends are the same as seen in ΔOASPL (fig. 12) but the magnitude is larger. Whereas the maximum value of ΔOASPL is about 10 dB, the maximum value of ΔL_A is about 25 dBA. This is not unexpected in light of the fact that the higher harmonics are much more affected by the wake than the first few harmonics. (See fig. 11.) Another difference is that behind the propeller disk ($\theta = 30°$), Twin 1 is no longer producing higher levels than Twin 3. Thus, both propeller designs are generating the same change of the high frequencies, whereas Twin 1 produced a greater change in the lower harmonics for $\theta = +30°$. (See fig. 12.)

The effect of the wake thickness on L_A is shown in figure 16. Again, the trends follow those seen for OASPL (fig. 13). However, the increases in L_A in going from $t/c = 0$ to $t/c = 1$ are much more pronounced particularly upstream and downstream ($\theta = \pm 30°$) of the propeller disk plane. This indicates that the higher frequencies are much more affected by the wake than the lower frequencies particularly for $\theta = \pm 30°$. Also, for the lower thrust loadings, L_A decreases with increasing wake thickness ($t/c = 1$ to $t/c = 3$). This decrease is understood in light of the fact that a thinner wake produces a narrower pulse in the acoustic signal and a narrower pulse has a higher frequency composition.

The dependence of ΔL_A on the angular location (θ) of the observer (microphone) with respect to the disk plane is shown in figure 17. The trends are similar to those seen in the ΔOASPL with the magnitude of the effects being much larger. Even at 90° to the airfoil, noise increases of about 20 dBA are calculated. Also of note

in the figure is the fact that the microphones which are outside the flow ($\phi = 77°$) are typically recording increases in L_A that are larger than inside the flow ($\phi = 25°$), particularly at $\theta = 0°$ (in the propeller disk plane). That is, the effect of the wake on the high frequencies is more pronounced at a position which is farther from the propeller.

SUMMARY OF RESULTS AND RECOMMENDATIONS

In this paper, the noise measured from a propeller operating in a wake was analyzed. Analysis of the data showed that, generally, the wake increased the overall noise (overall sound pressure level (OASPL)) produced by the propeller; increased the harmonic content of the noise, thus the scaled A-weighted sound level L_A; and produced an azimuthal dependence. When the effects of the propeller thrust, wake thickness, and observer location on ΔOASPL and OASPL were examined, the following observations were made. The ΔOASPL decreased with increasing propeller thrust. The OASPL increased as the wake thickness increased but the major part of the increase was observed between thickness-chord ratios (t/c) of 0 and 1. Little additional noise increase resulted between $t/c = 1$ and $t/c = 3$. The highest values of ΔOASPL were found at observer locations corresponding to 25° from the plane of the wake ($\phi = 25°$) and out of the plane of the propeller disk ($\theta = \pm 30°$). The maximum value of ΔOASPL was about 10 dB. The lowest values of ΔOASPL were observed in the disk plane and normal to the plane of the wake.

The effects of the wake on the scaled L_A were also studied, and the effects were similar to those on OASPL with two exceptions. First, the magnitude of the increases in the noise level ΔL_A were much larger. The maximum value of ΔL_A was 25 dBA. This large increase reflects the large change in the frequency content of the acoustic signal when the wake is introduced. The other exception is that in certain cases, ΔL_A decreases when t/c was increased from 1 to 3. A thicker wake produces a wider pulse in the acoustic signal which has a lower frequency content.

Finally, both propellers produced the same trends in ΔOASPL and ΔL_A with thrust and wake thickness. Twin 1, however, had consistently higher ΔOASPL values downstream of the propeller ($\theta = +30°$).

The increases in noise produced by a wake entering a propeller have been shown to have strong directional characteristics. Further study should involve a measurement scheme which can map out the directivity in both the directions of θ and ϕ in more detail. A knowledge of these directivity patterns could aid in minimizing the noise impact of a propeller operating in a wake.

The study described herein was limited to a relatively low forward speed as far as aircraft operations are concerned. Extension to higher speeds would complete the current data base.

Langley Research Center
National Aeronautics and Space Administration
Hampton, VA 23665
August 30, 1984

REFERENCES

1. Mitchell, Glenn A.; and Mikkelson, Daniel C.: Summary of Recent Results From the NASA Advanced High-Speed Propeller Research Program. NASA TM-82891, 1982.

2. Herkes, W.: An Experimental Study of the Noise Generated by a Pusher Propeller Due to a Wake Entering the Propeller Disc. EOARD TR-80-5 (Contract AFOSR 79-0033), Nov. 5, 1979. (Available from DTIC as AD A078 437.)

3. Connor, Andrew B.; Hilton, David A.; and Dingeldein, Richard C.: Noise Reduction Studies for the Cessna Model 337 (O-2) Airplane. NASA TM X-72641, 1975.

4. Block, P. J. W.: Noise Generated by a Propeller in a Wake. NASA TM-85794, 1984.

5. Block, Patricia J. W.; and Martin, Ruth M.: Results From Performance and Noise Tests of Model Scale Propellers. SAE Tech. Paper Ser. 830730, Apr. 1983.

6. Block, P. J. W.: Operational Evaluation of a Propeller Test Stand in the Quiet Flow Facility at Langley Research Center. NASA TM-84523, 1982.

7. Hubbard, Harvey H.; and Manning, James C.: Aeroacoustic Research Facilities at NASA Langley Research Center - Description and Operational Characteristics. NASA TM-84585, 1983.

TABLE 1.- MICROPHONE COORDINATES

Mic	Coordinate						Distance		Relative position with respect to -	
	x_1		x_2		x_3		$\sqrt{x_1^2 + x_2^2 + x_3^2}$		Disk plane, θ, deg (a)	Airfoil, ϕ, deg
	in.	m	in.	m	in.	m	in.	m		
3a	16.3	0.414	7.6	0.193	9.0	0.229	20.1	0.511	-30	25
3b	16.3	.414	7.6	.193	.0	.000	18.0	.457	0	25
3c	16.3	.414	7.6	.193	-9.0	-.229	20.1	.511	+30	25
3d	.0	.000	18.0	.457	9.0	.229	20.1	.511	-30	90
3e	.0	.000	18.0	.457	.0	.000	18.0	.457	0	90
3f	.0	.000	18.0	.457	-9.0	-.229	20.1	.511	+30	90
4	-8.23	-.209	-35.7	-.906	18.3	.465	40.9	1.04	-30	77
5	-8.23	-.209	-35.7	-.906	.0	.000	36.6	.931	0	77
6	-8.23	-.209	-35.7	-.906	-18.3	-.465	40.9	1.04	+30	77

[a]A minus sign indicates upstream of the propelller disk; a plus sign indicates downstream of the propeller disk.

TABLE 2.- SUMMARY OF TEST CONDITIONS FOR PERFORMANCE MEASUREMENTS

Propeller		In flow		
Type	$\beta_{.75}$, deg	No wake	With wake	
			t/c = 1	t/c = 3
Twin 1	16	x	x	
	20	x	x	x *
	24	x	x	x
	28	x	x	x
	32	x	x	x
	36	x	x	x
	40	x	x	
Twin 3	15	x	x	x *
	16	x	x	
	20	x	x	x *
	24	x	x	x
	28	x	x	x
	32	x	x	x
	36	x	x	x

*Noise measurements were made at these conditions.

TABLE 3.- SUMMARY OF TEST CONDITIONS FOR NOISE MEASUREMENT

Propeller	$\beta_{.75}$, deg	Airfoil, angle of attack, deg	T_A		ρ_A		Rotational speed, rpm	Thrust		C_T	C_P	J	M_T
			°F	°C	slugs/ft^3	kg/m^3		lbf	N				
Twin 1	20	----	74.0	23.3	0.0025	1.2884	5250	40	178	0.089	0.075	0.614	0.550
		15.0	75.0	23.9	.0025	1.2884	5165			.092	.076	.626	.538
		20.4	74.8	23.8	.0025	1.2884	5100			.095	.078	.636	.531
	20	----	74.0	23.3	0.0025	1.2884	6565	83	369	0.117	0.091	0.501	0.680
		15.0	74.8	23.8	.0025	1.2884	6485			.120	.092	.503	.670
		20.4	74.5	23.6	.0025	1.2884	6469			.120	.093	.502	.670
Twin 3	20	----	77.0	25.0	0.00247	1.2730	5160	40	178	0.094	0.081	0.631	0.536
		15.0	72.3	22.4	.0025	1.2884	5080			.096	.084	.642	.531
		20.4	73.2	22.9	.0025	1.2884	5070			.096	.081	.642	.529
	20	----	77.0	25.0	0.00247	1.2730	6510	83	369	0.119	0.093	0.502	0.672
		15.0	72.7	22.6	.0025	1.2884	6460			.120	.094	.508	.670
		20.4	75.6	24.2	.00247	1.2730	6460			.122	.093	.506	.668
	15	----	74.7	23.6	0.0025	1.2884	7810	100	445	0.099	0.067	0.420	0.805
		15.0	74.7	23.6	.00248	1.2781	7789			.100	.067	.423	.803
		20.4	75.2	24.0	.00248	1.2781	7768			.101	.066	.420	.800

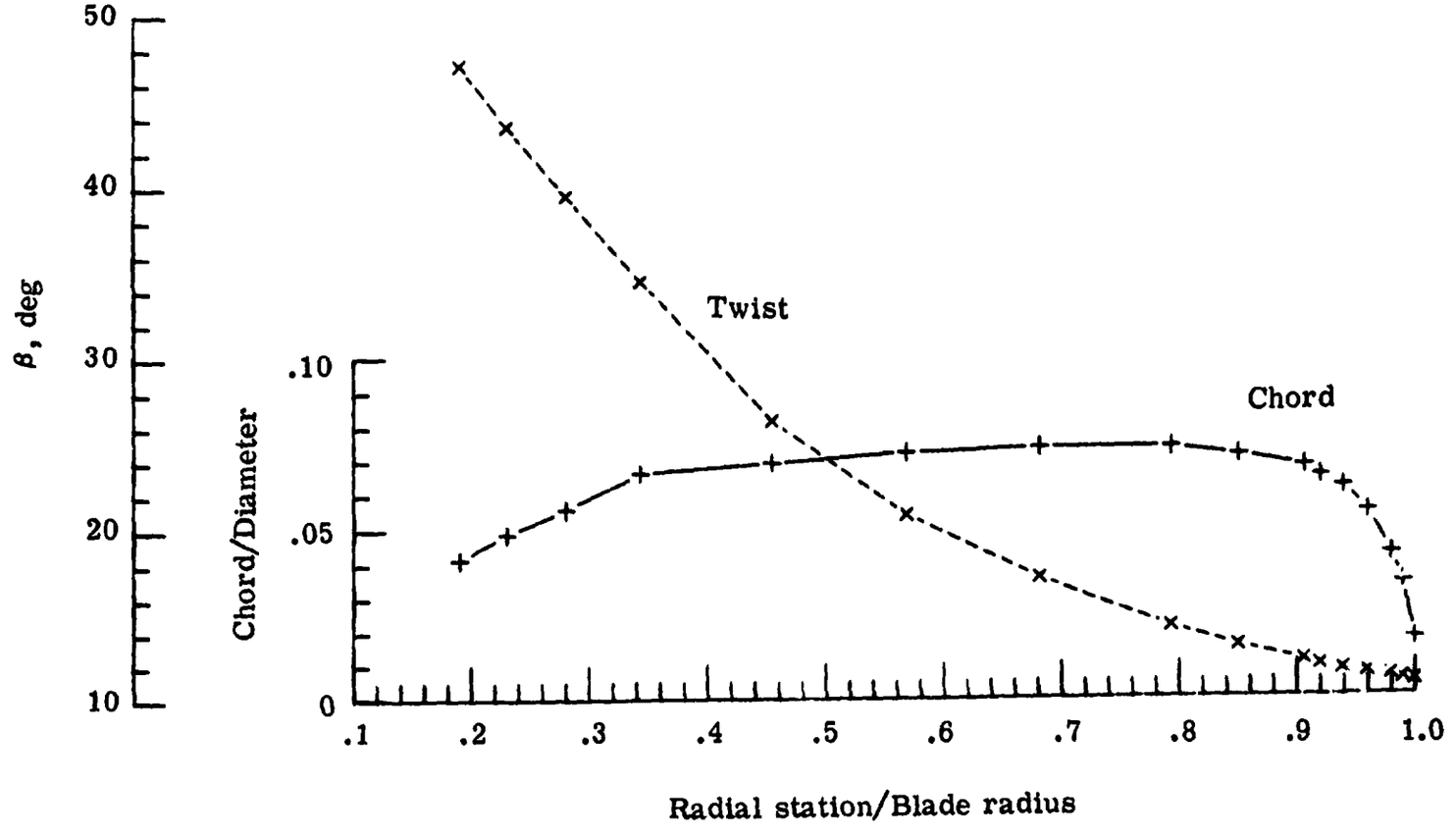

(a) Chord and twist distribution.

Figure 1.- Description of Twin 1 propeller.

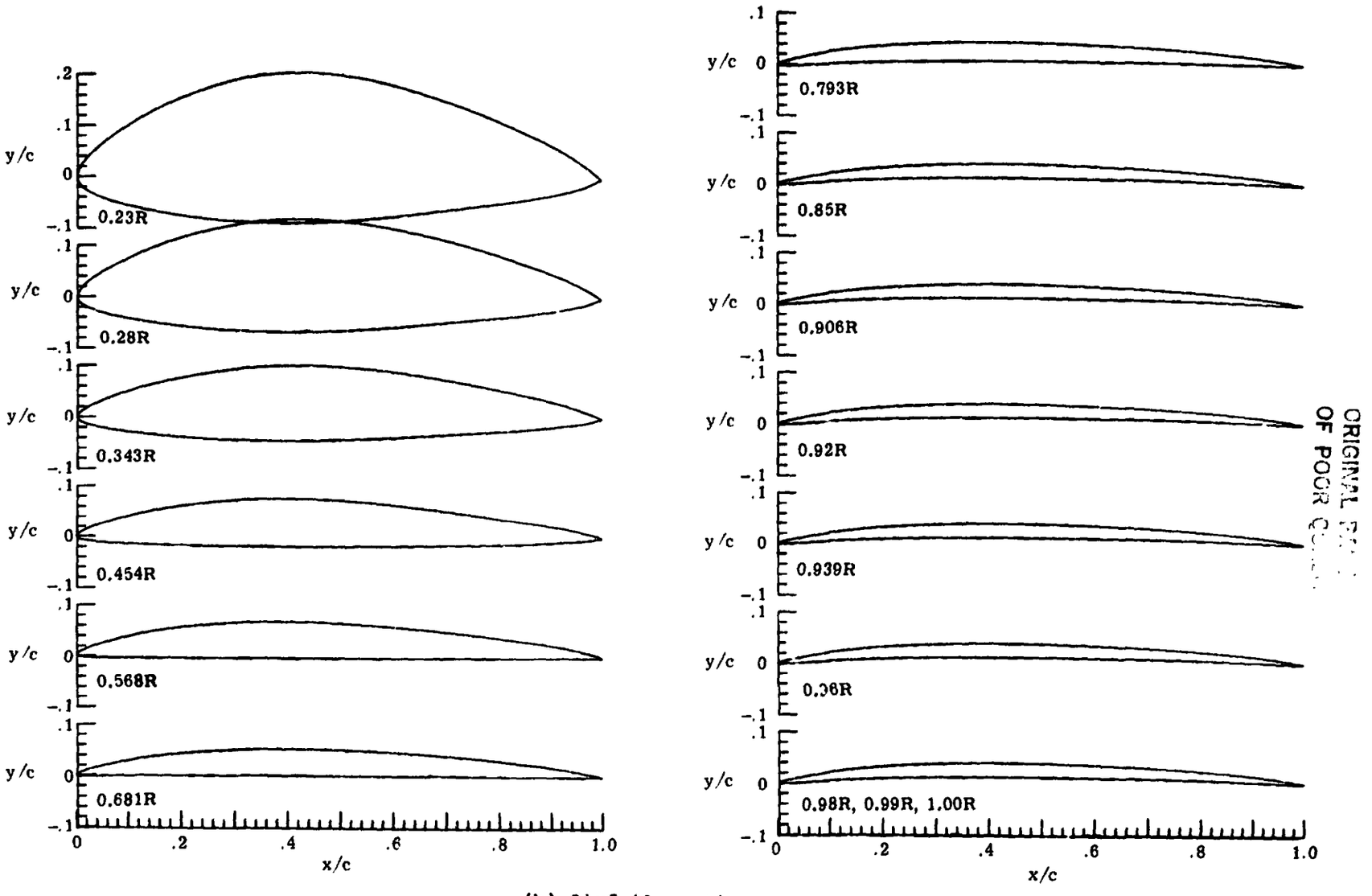

(b) Airfoil sections.

Figure 1.- Concluded.

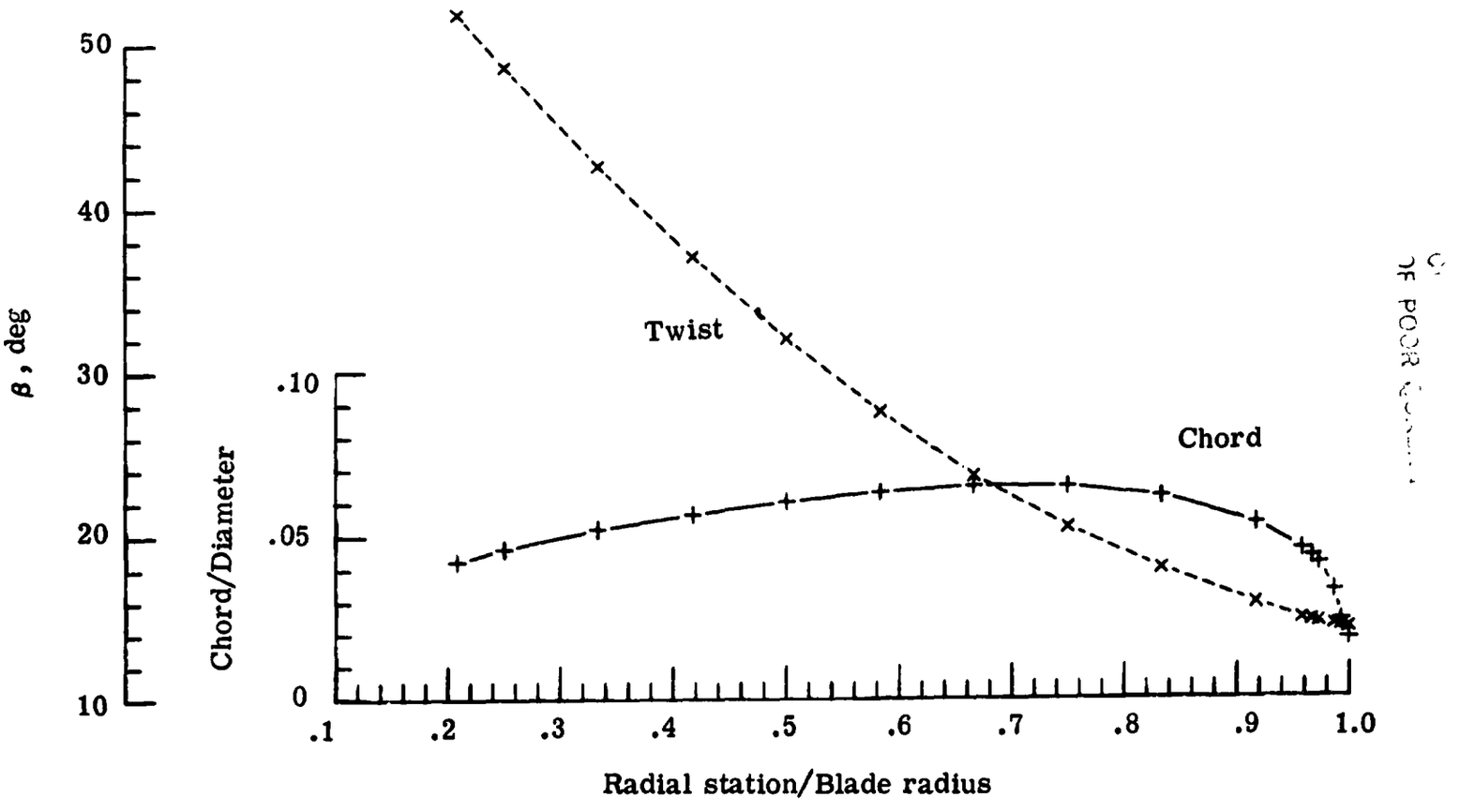

(a) Chord and twist distribution.

Figure 2.- Description of Twin 3 propeller.

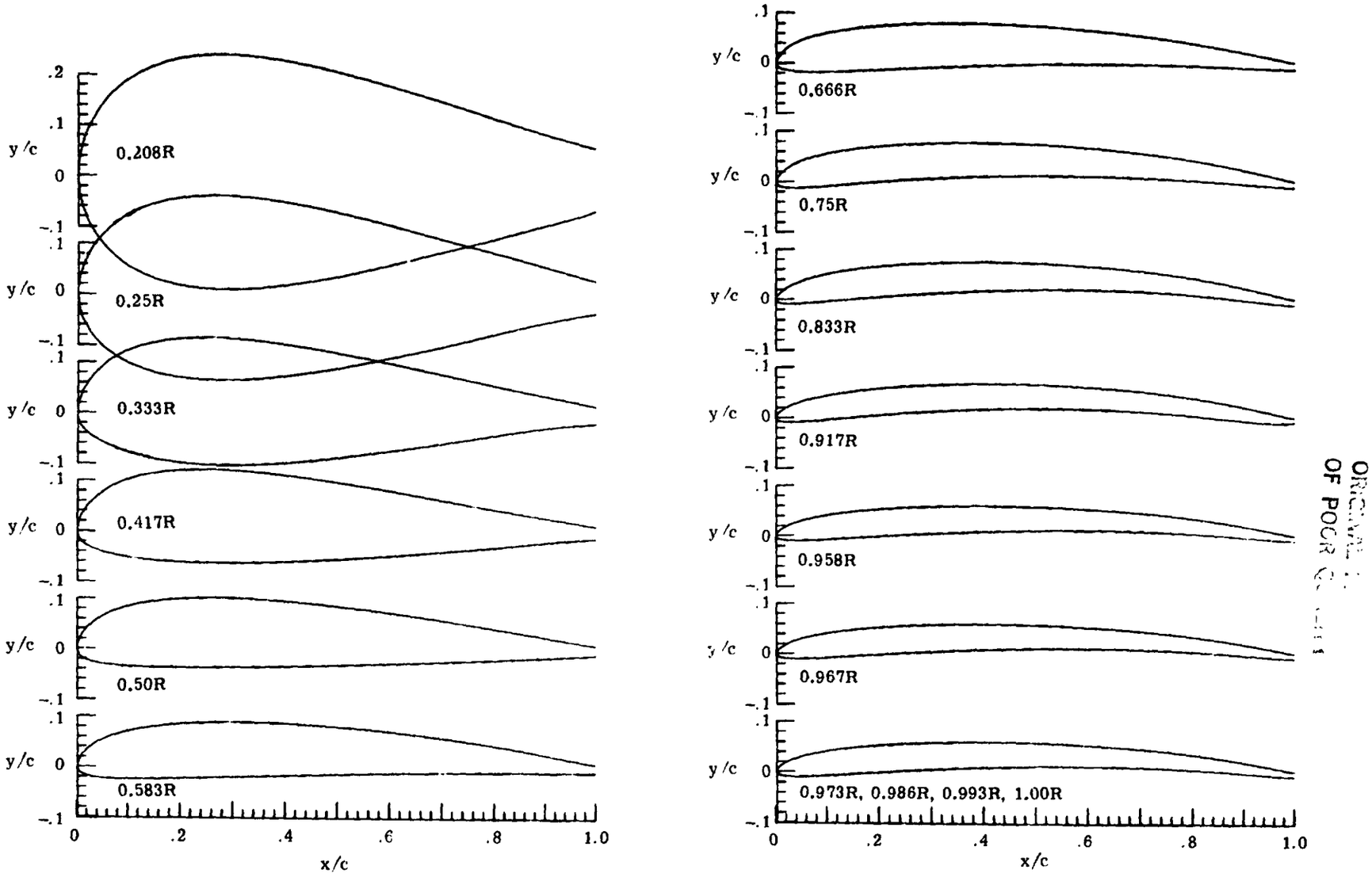

(b) Airfoil sections.

Figure 2.- Concluded.

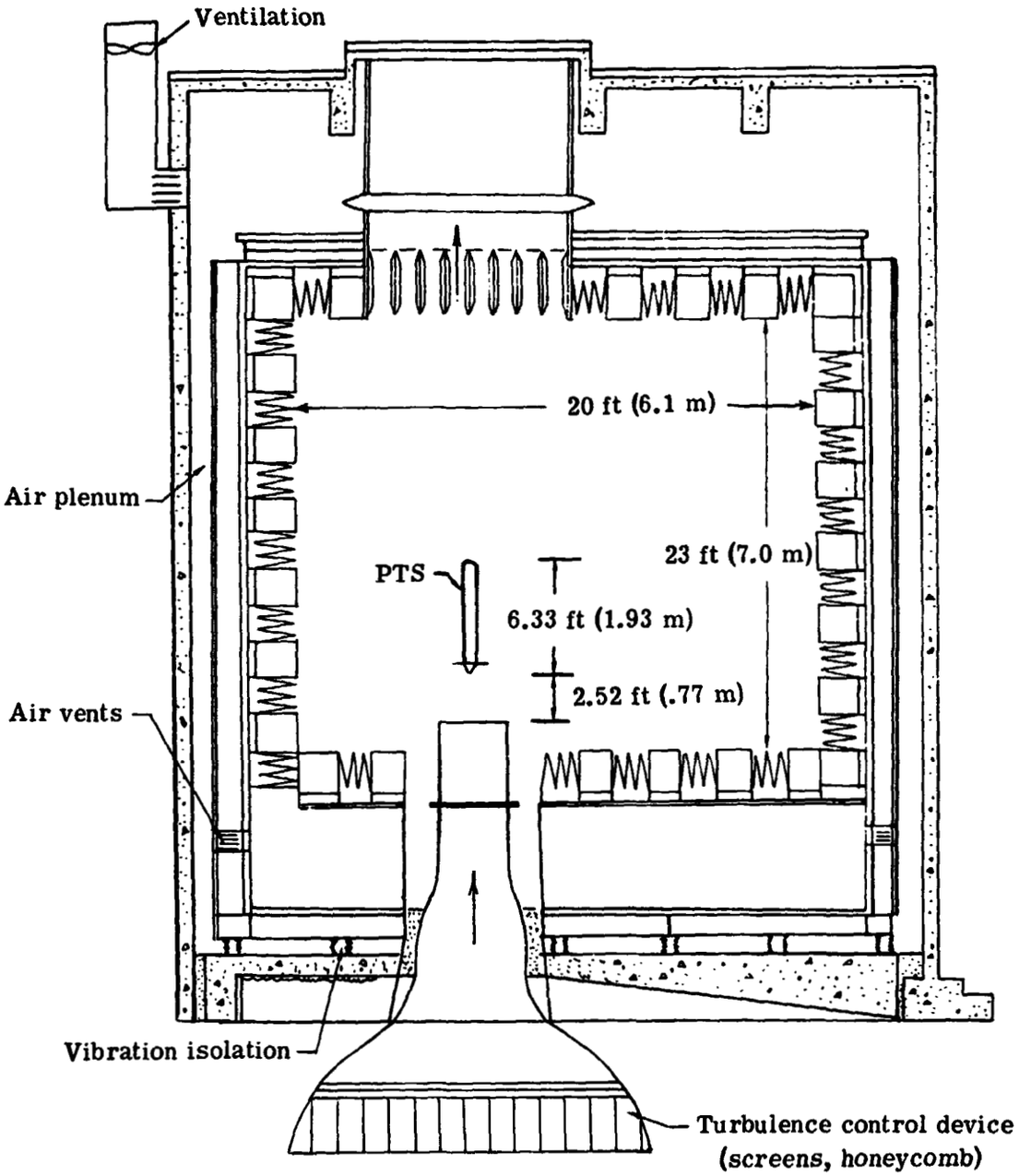

Figure 3.- Schematic of propeller test stand in quiet flow facility.

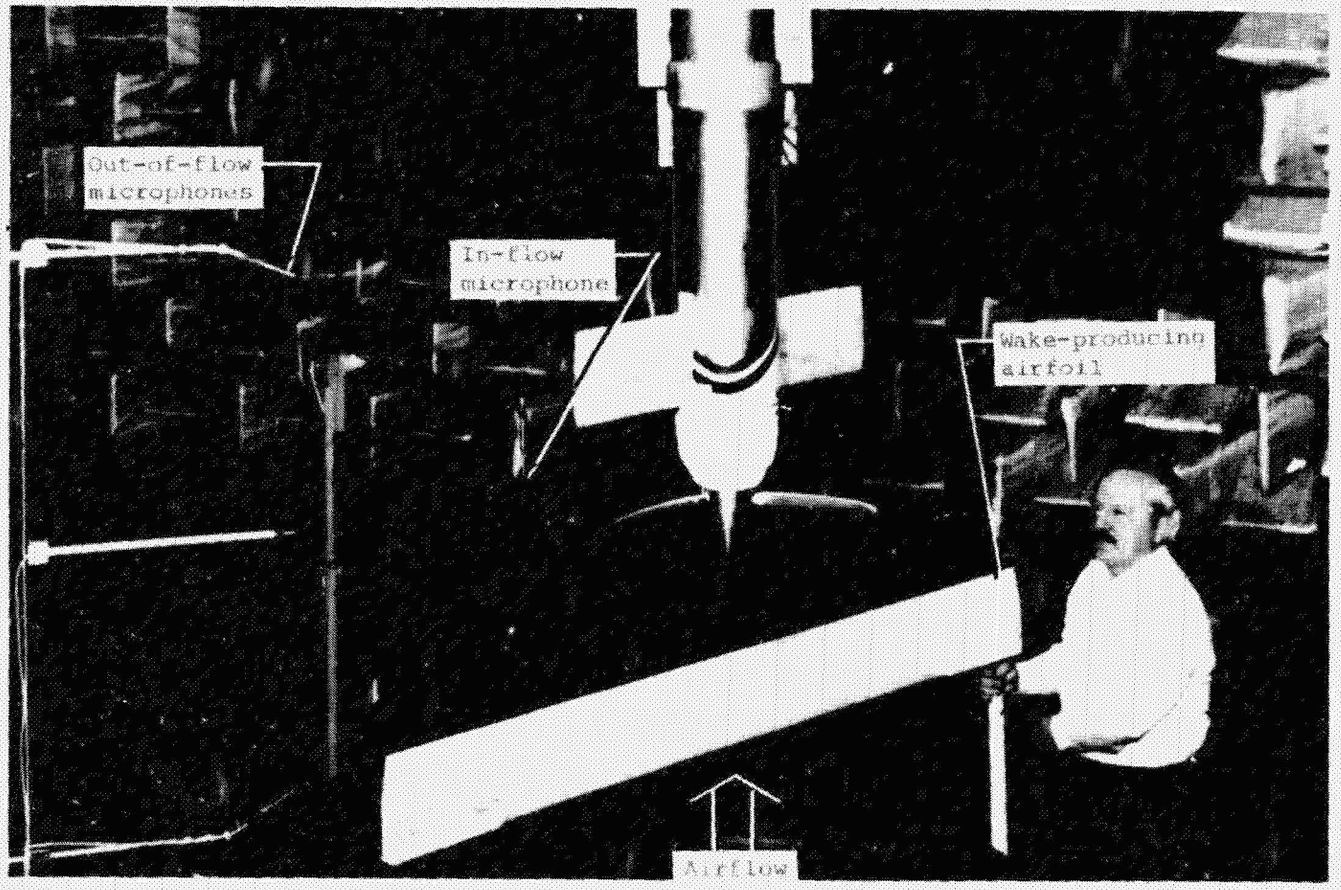

L-84-120

Figure 4.- Wake-producing airfoil upstream of propeller disk.

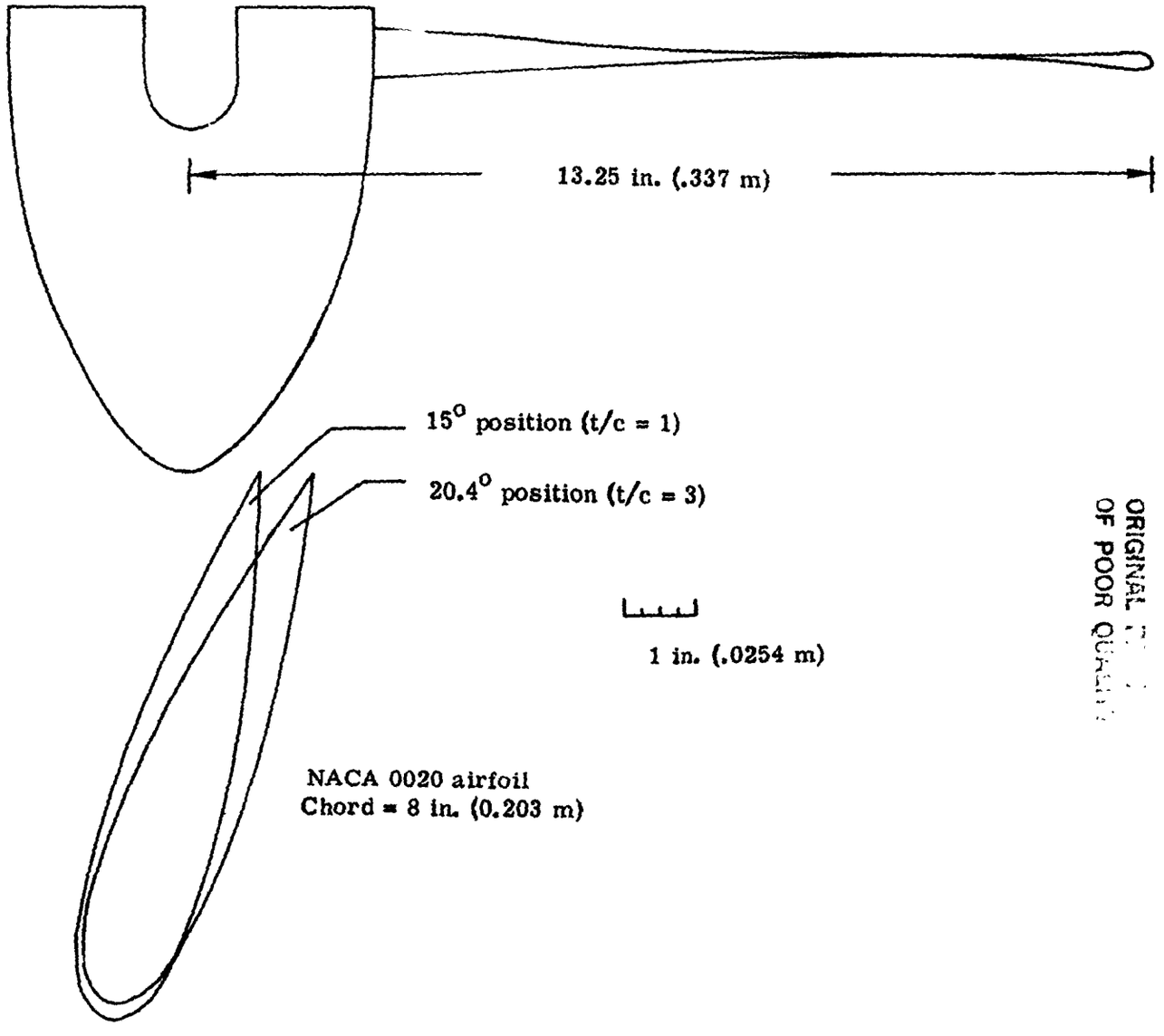

Figure 5.- Scale drawing showing positions and dimensions of NACA 0020 airfoil used for producing wake.

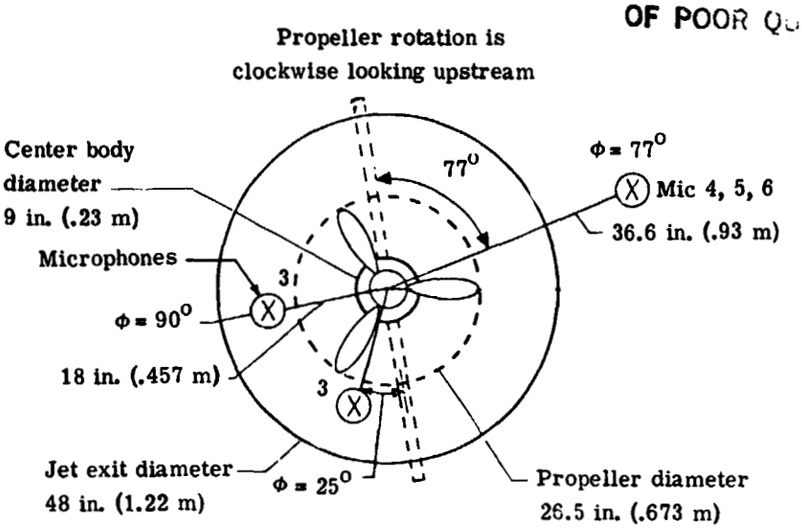

Plan view

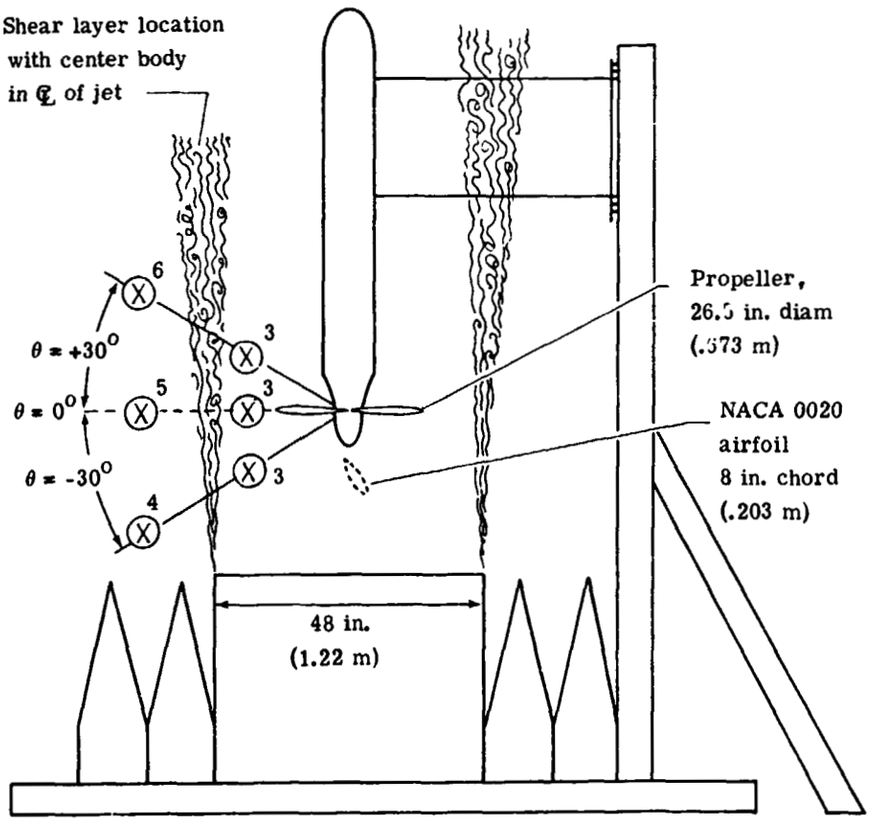

Side view with microphones 4, 5, and 6 shown in line with 3

Figure 6.- Schematic of test setup.

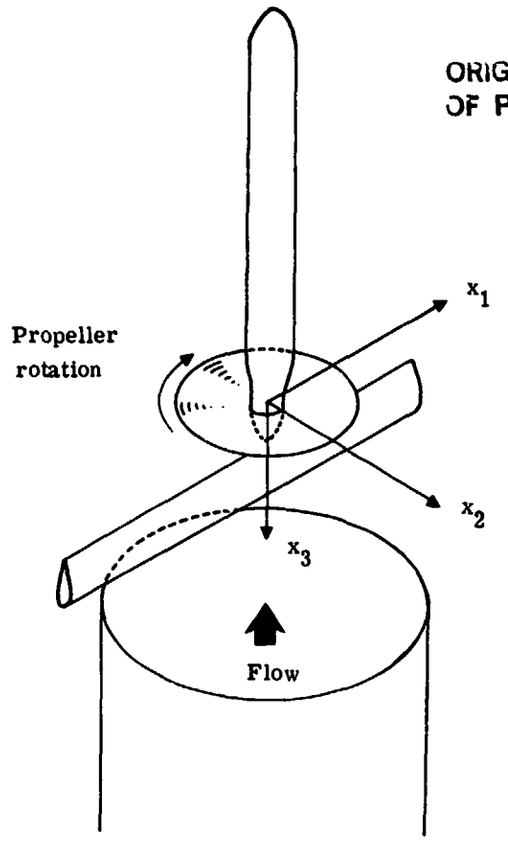

Figure 7.- Isometric drawing showing coordinate system in which microphone locations are defined.

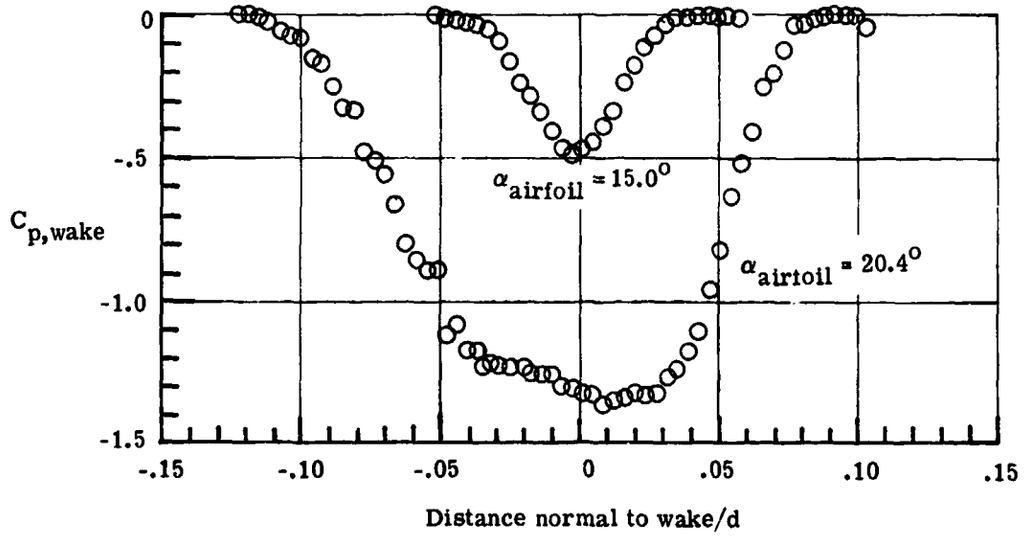

Figure 8.- Results from wake survey showing velocity defect region produced by airfoil. U = 118.7 fps (36.2 m/s).

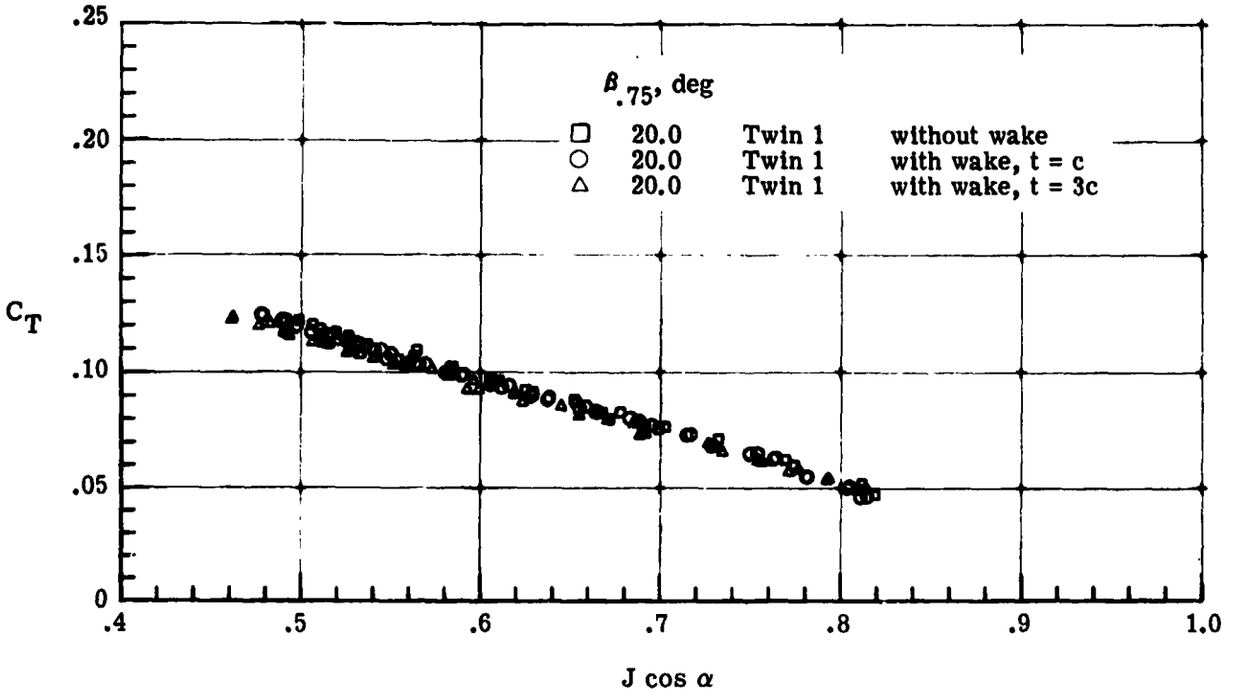

(a) Thrust coefficient.

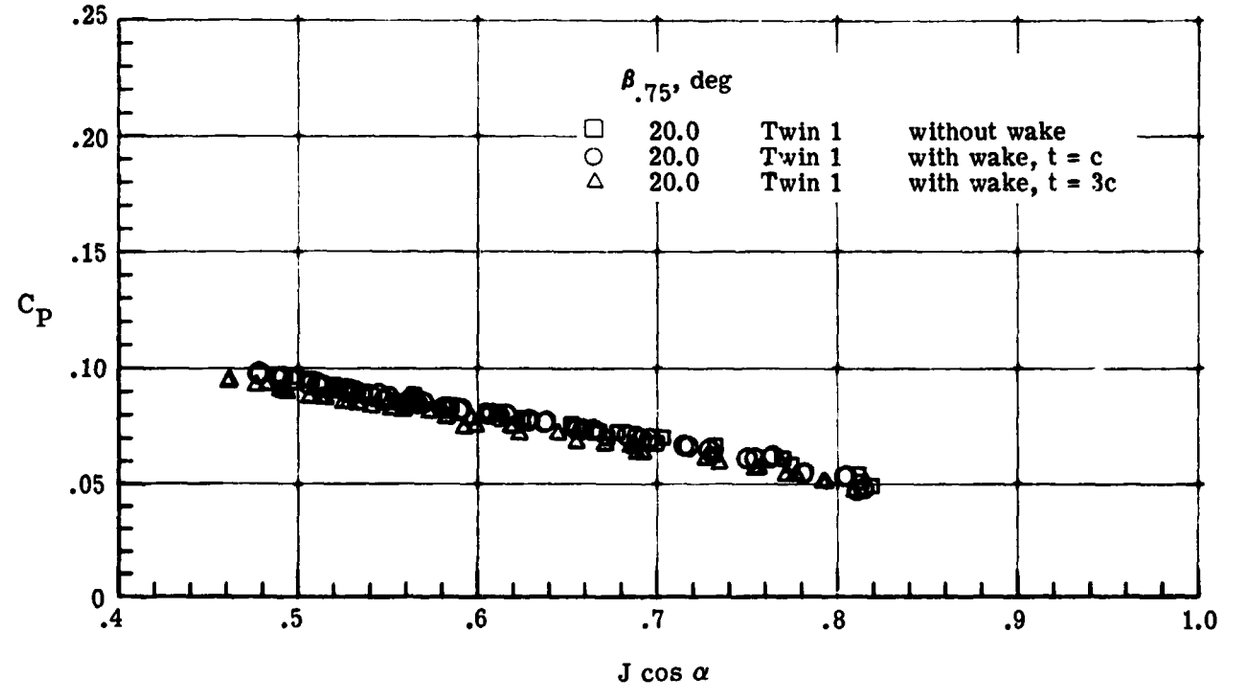

(b) Power coefficient.

Figure 9.- Performance characteristics for Twin 1 propeller.

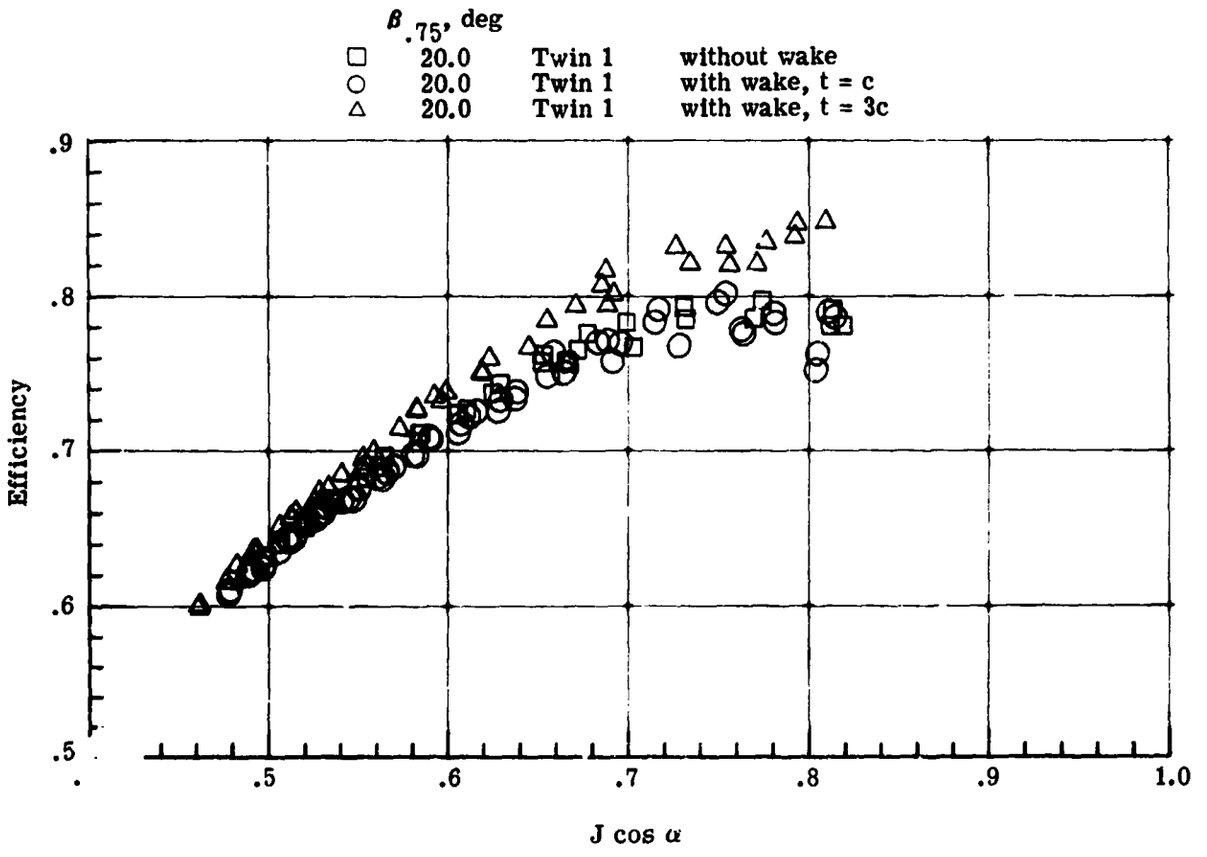

(c) Efficiency.

Figure 9.- Concluded.

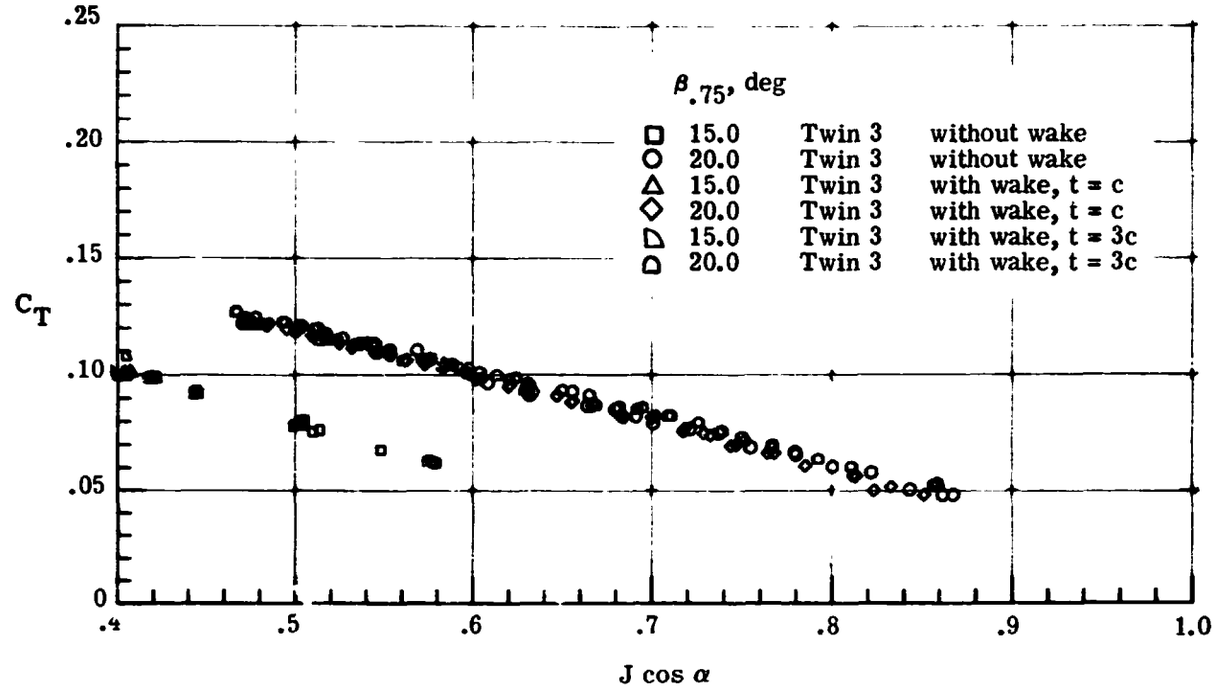

(a) Thrust coefficient.

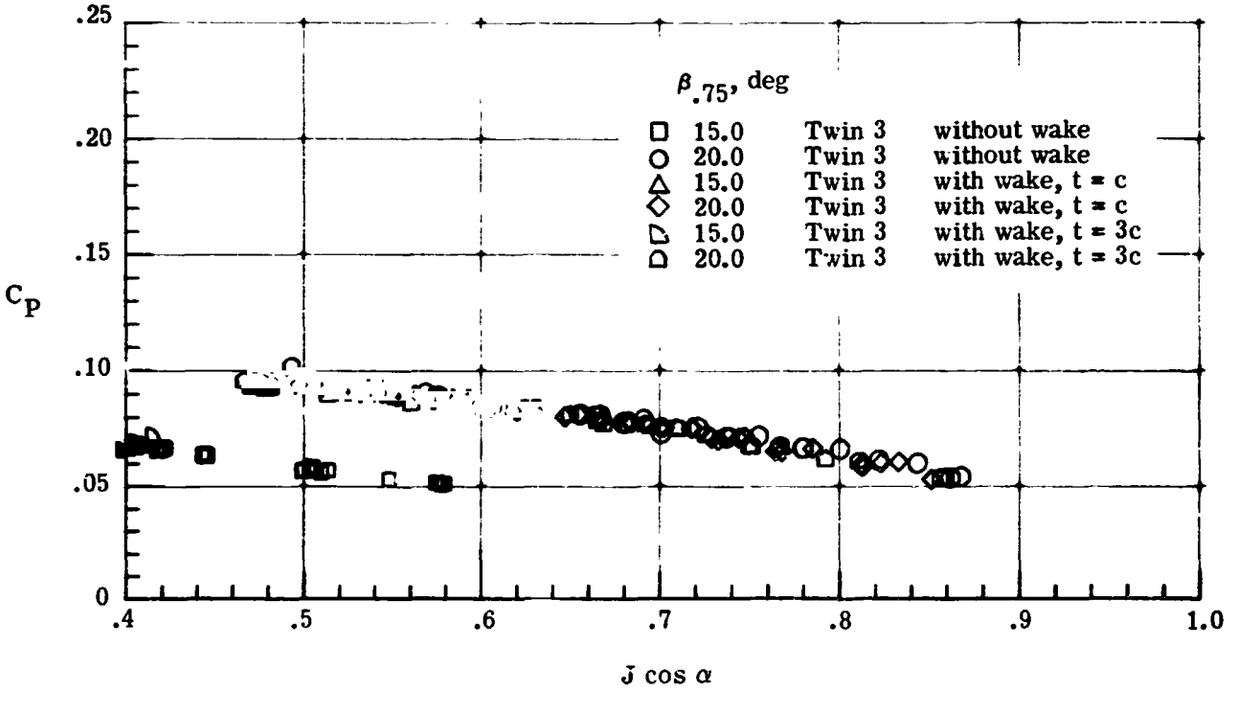

(b) Power coefficient.

Figure 10.- Performance characteristics for Twin 3 propeller.

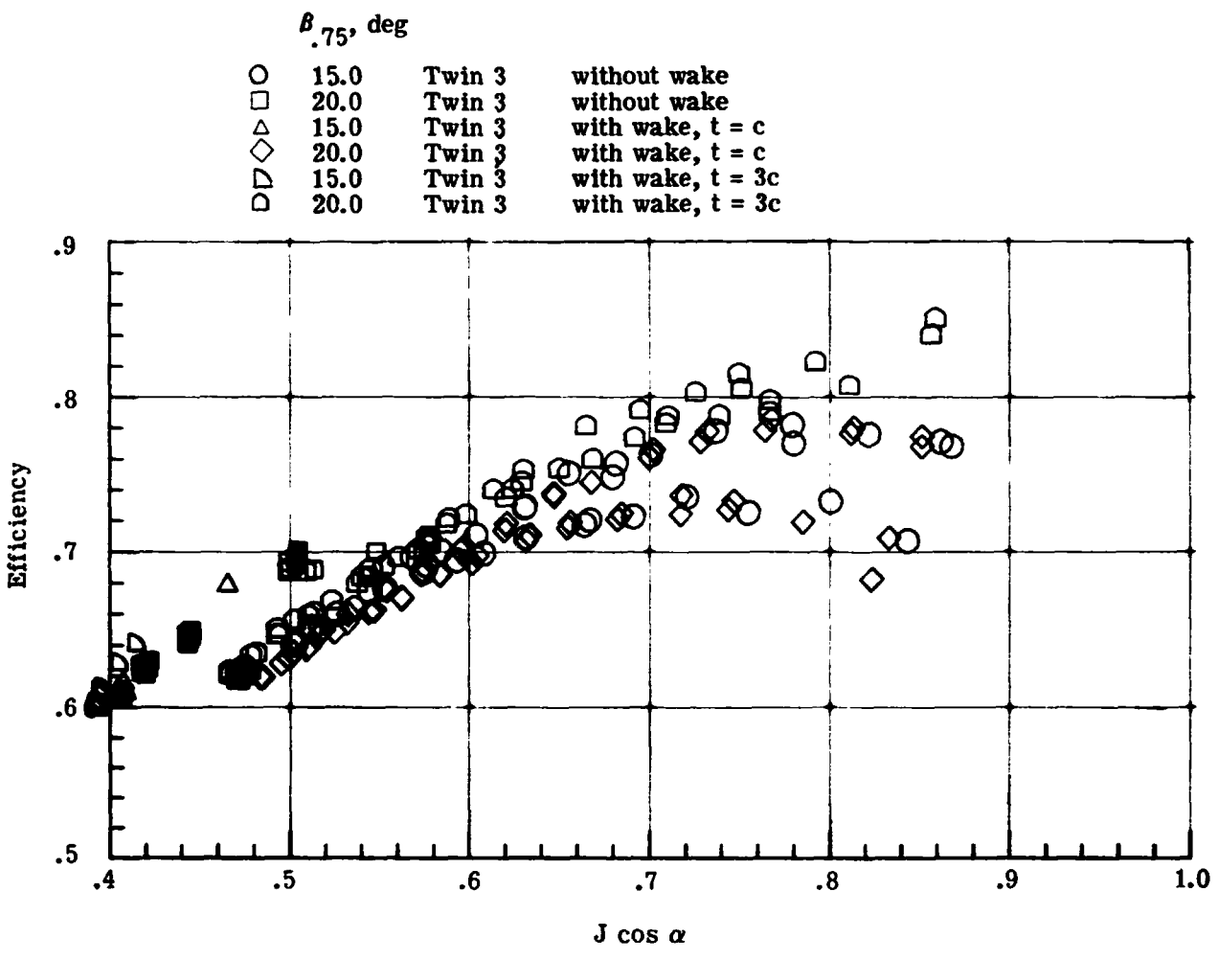

(c) Efficiency.

Figure 10.- Concluded.

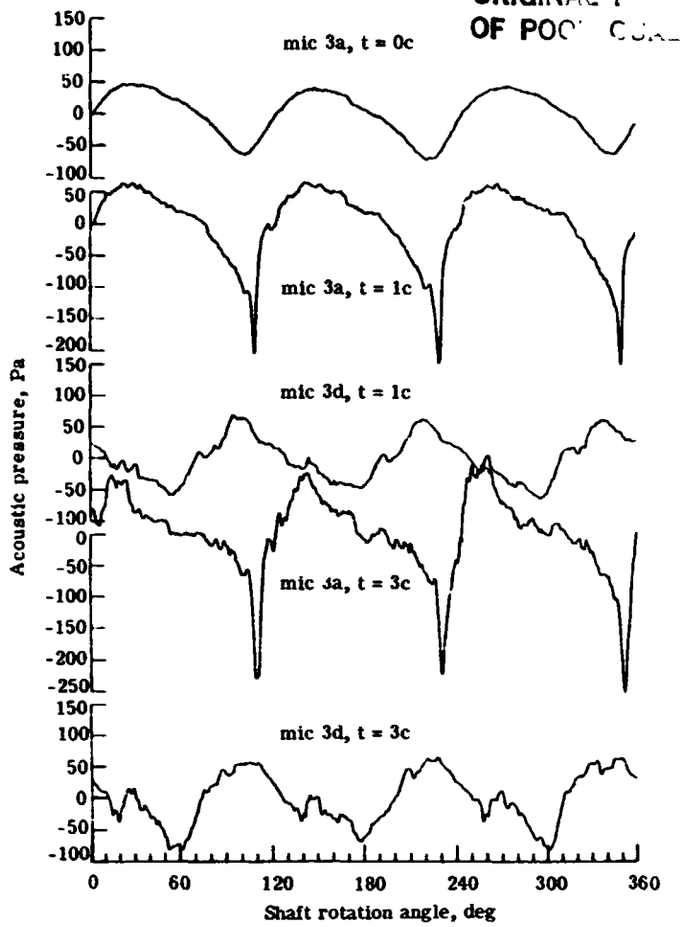

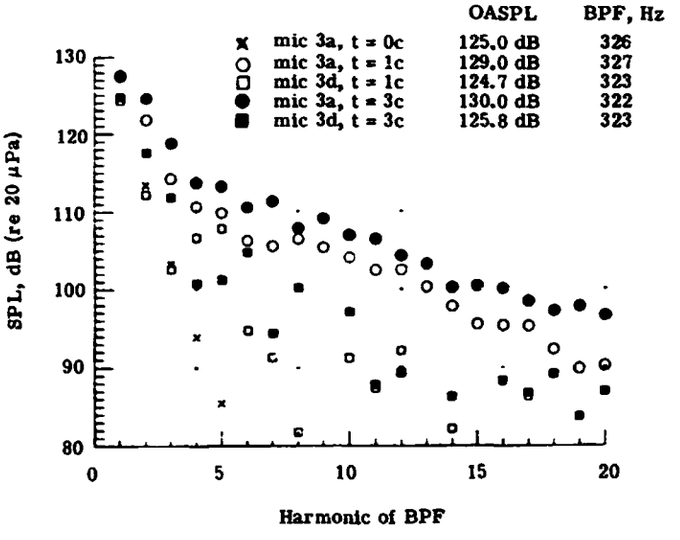

Figure 11.- Typical data set from reference 4. Twin 1; $\beta_{.75} = 20°$; thrust, 83 lbf (369 N); microphone 3; $\theta = -30°$.

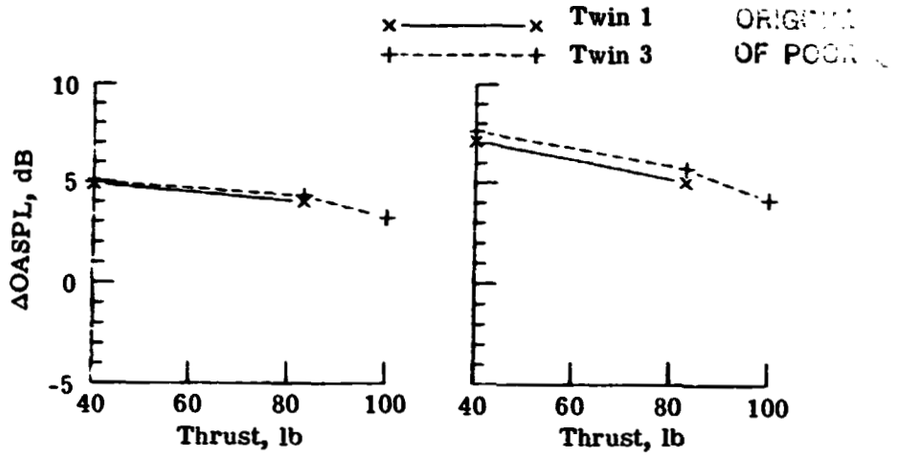

(a) Microphone 3a.

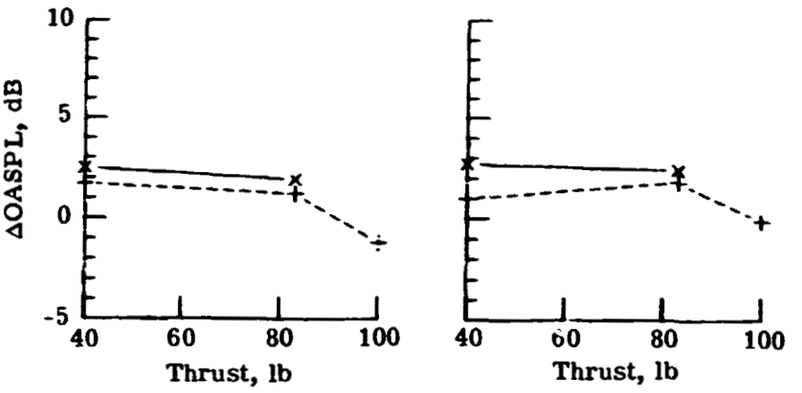

(b) Microphone 3b.

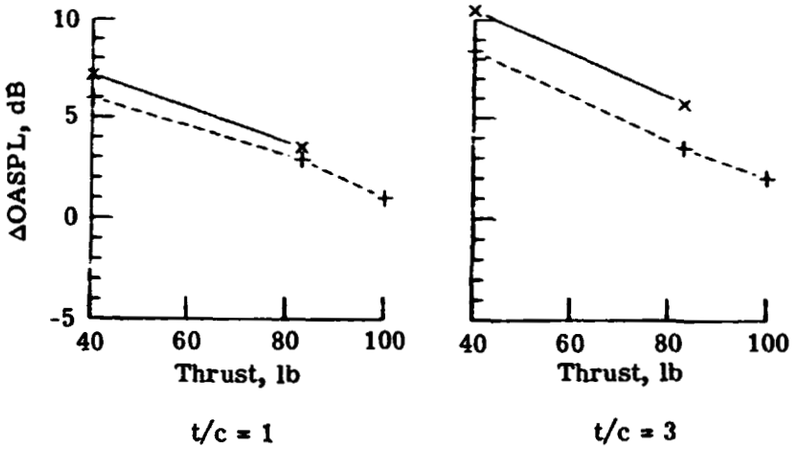

(c) Microphone 3c.

Figure 12.- Effect of propeller thrust on noise produced by propeller in wake. (1 lb = 4.45 N.)

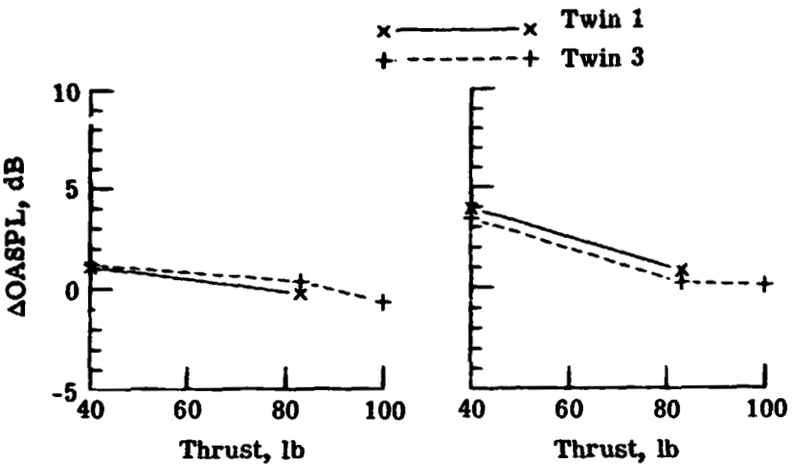

(d) Microphone 3d.

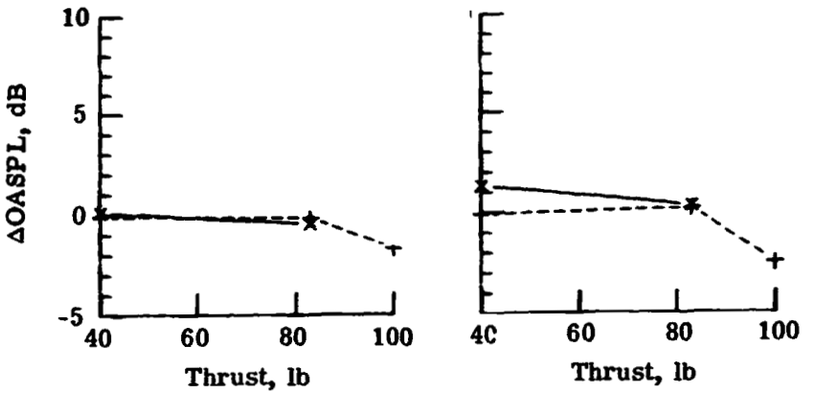

(e) Microphone 3e.

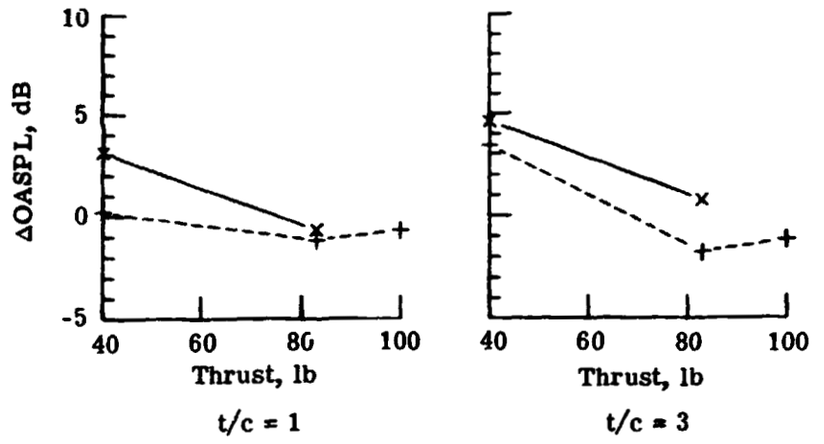

(f) Microphone 3f.

Figure 12.- Continued.

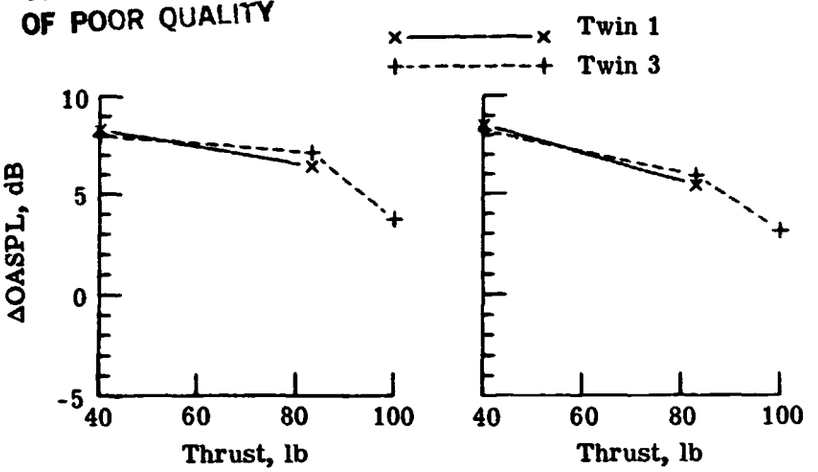

(g) Microphone 4.

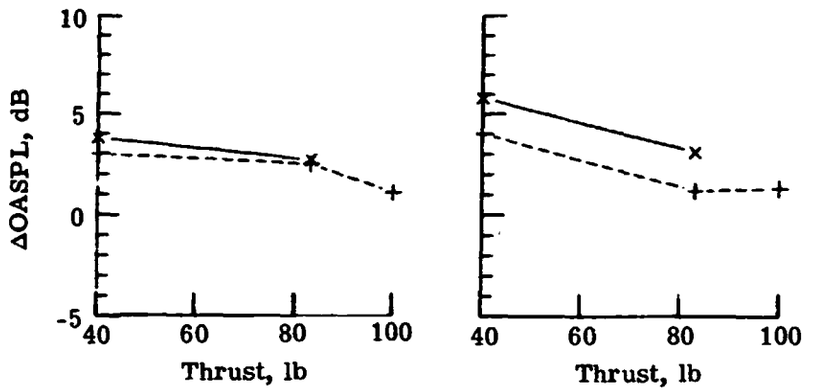

(h) Microphone 5.

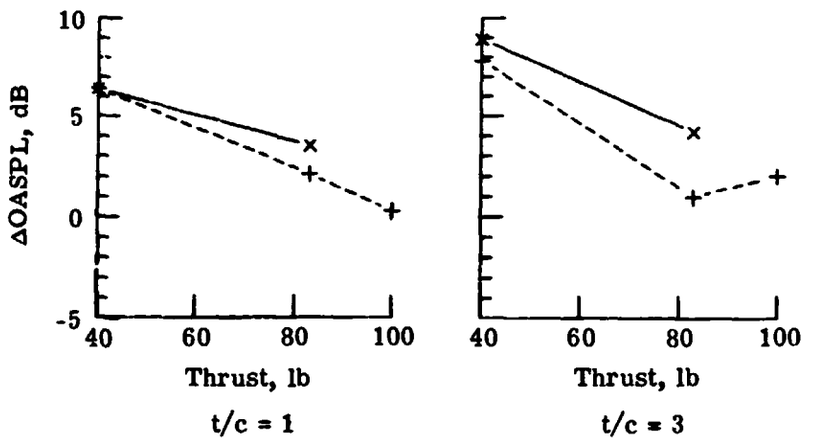

(i) Microphone 6.

Figure 12.- Concluded.

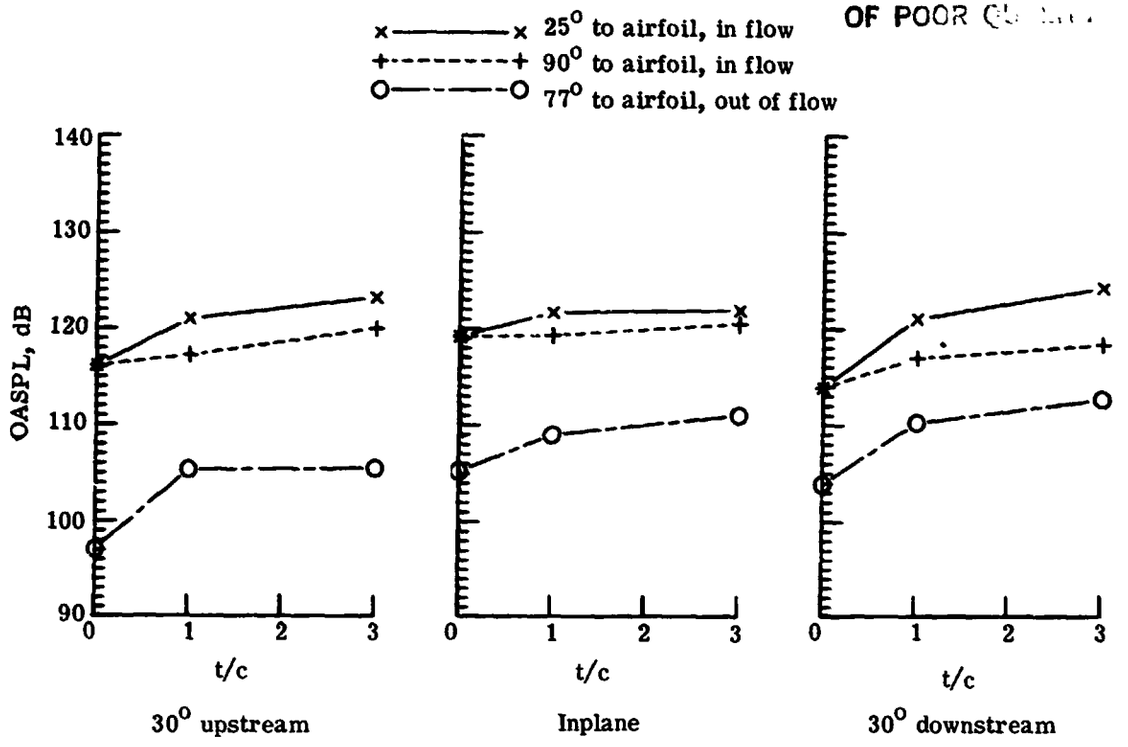

(a) Twin 1; $\beta_{.75}$ = 20°; T = 40 lb (178 N).

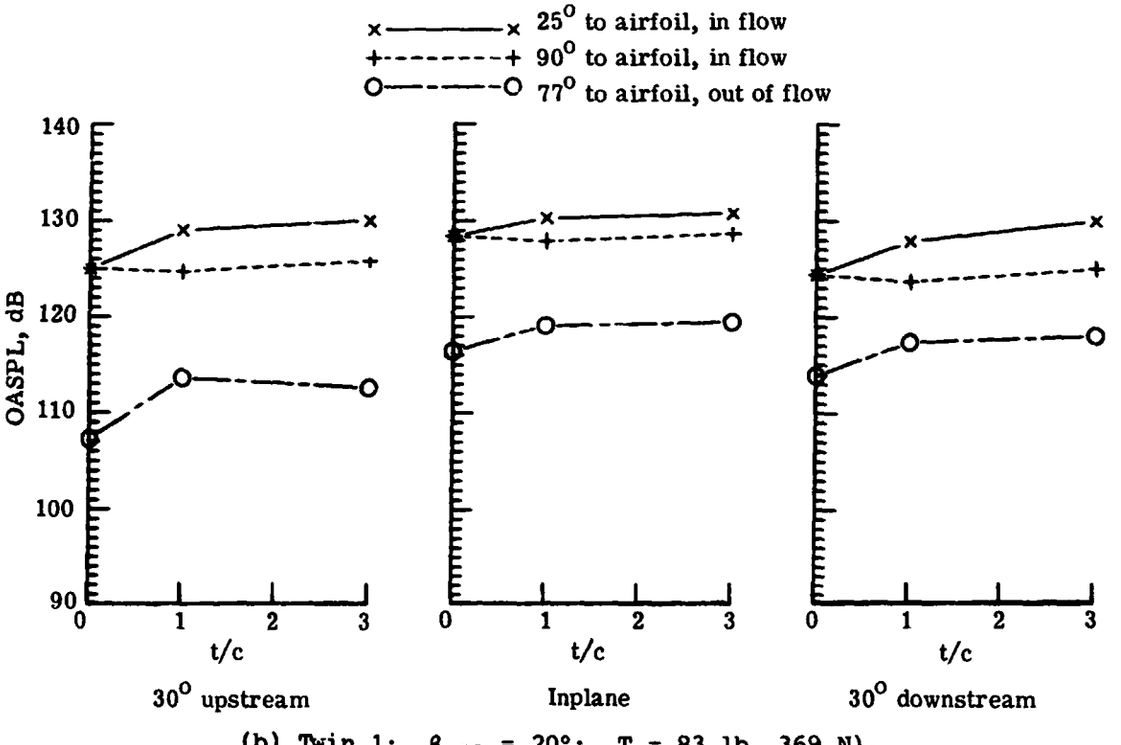

(b) Twin 1; $\beta_{.75}$ = 20°; T = 83 lb .369 N).

Figure 13.- Effect of wake thickness on noise produced by propeller in wake.

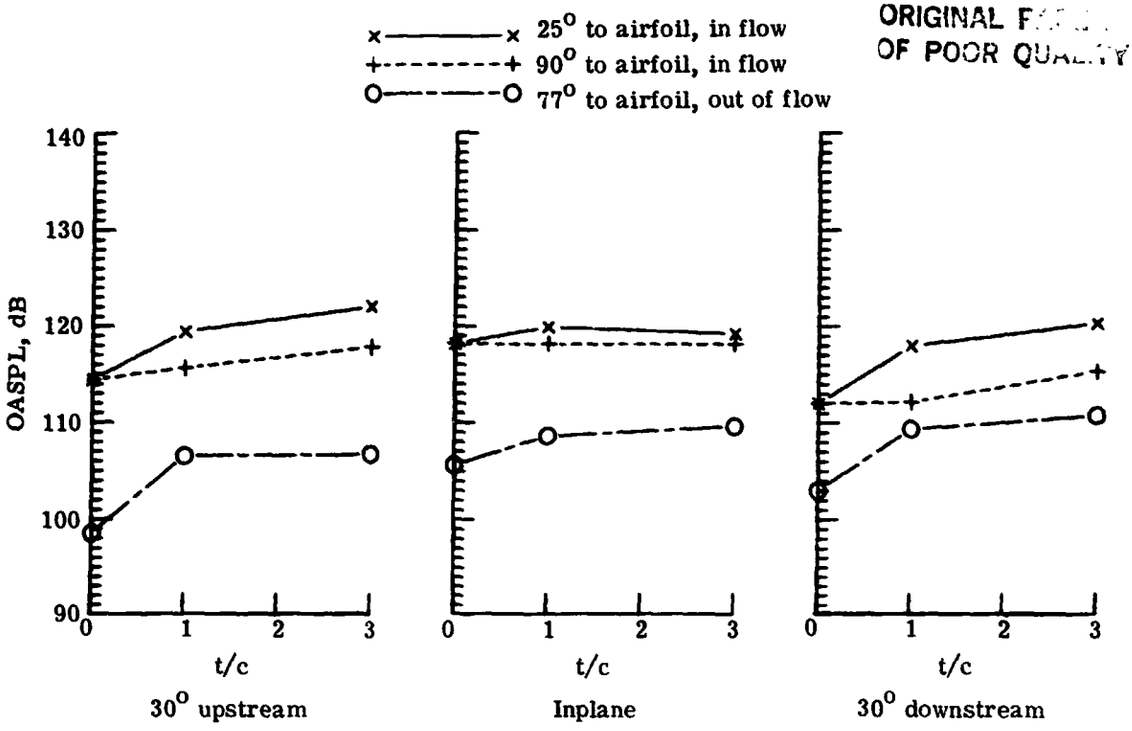

(c) Twin 3; $\beta_{.75}$ = 20°; T = 40 lb (178 N).

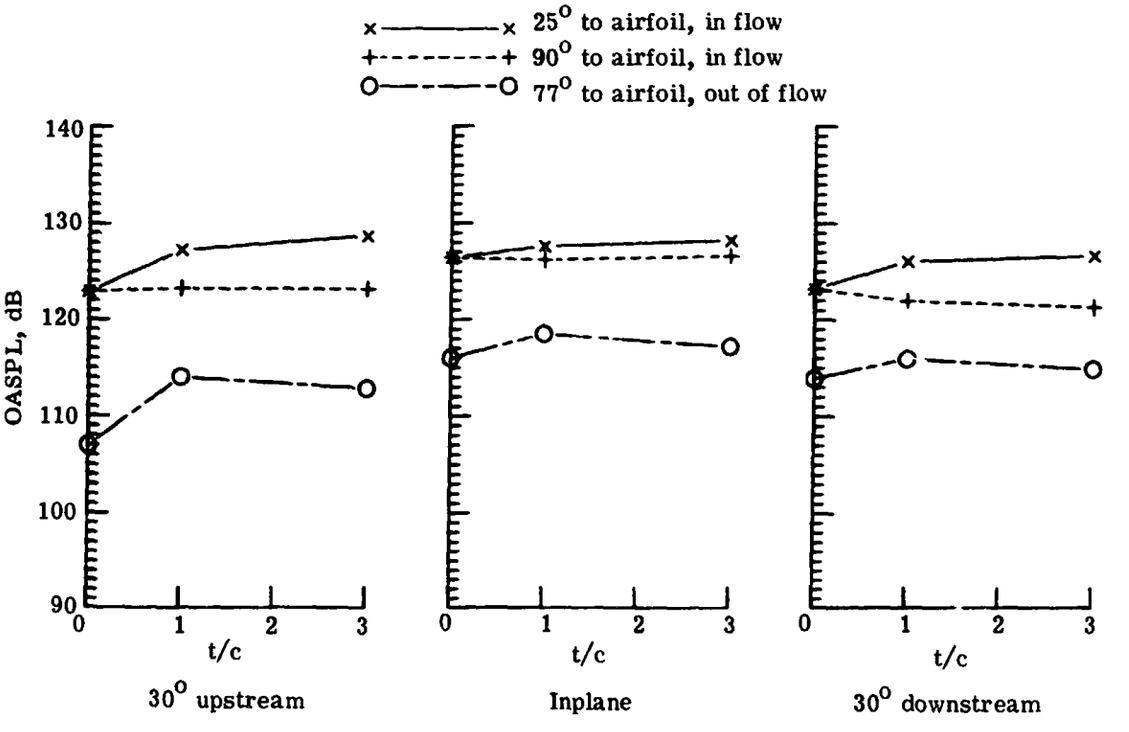

(d) Twin 3; $\beta_{.75}$ = 20°; T = 83 lb (369 N).

Figure 13.- Continued.

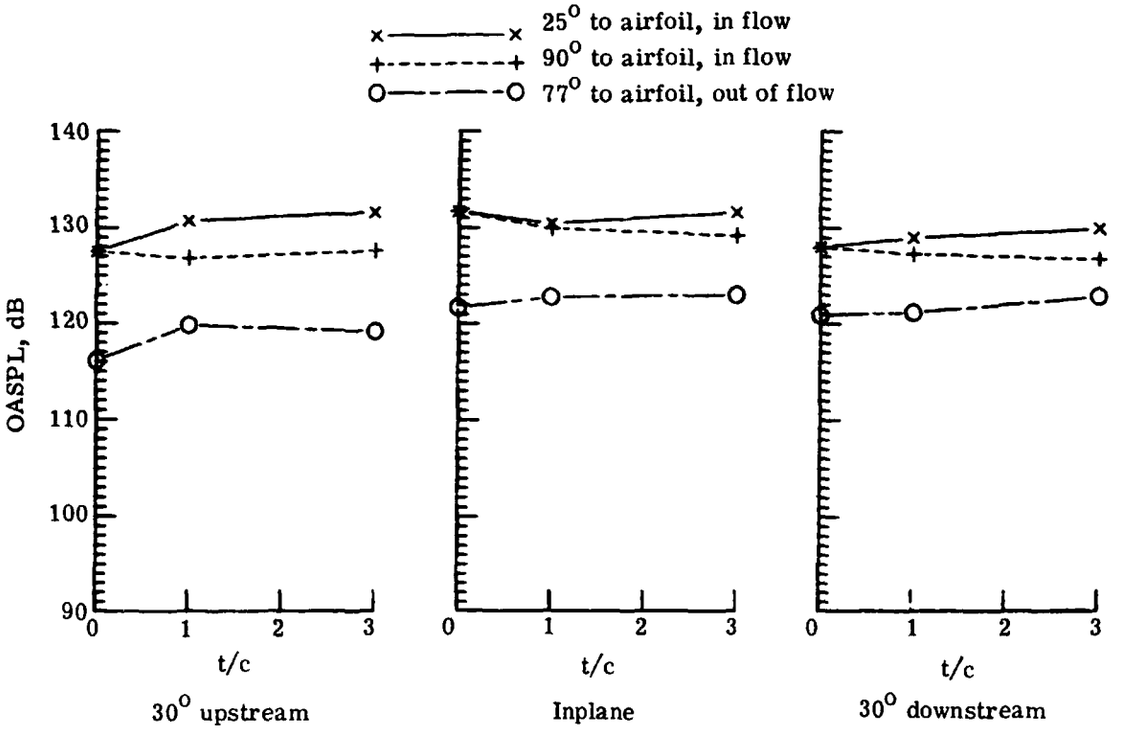

(e) Twin 3; $\beta_{.75}$ = 15°; T = 100 lb (445 N).

Figure 13.- Concluded.

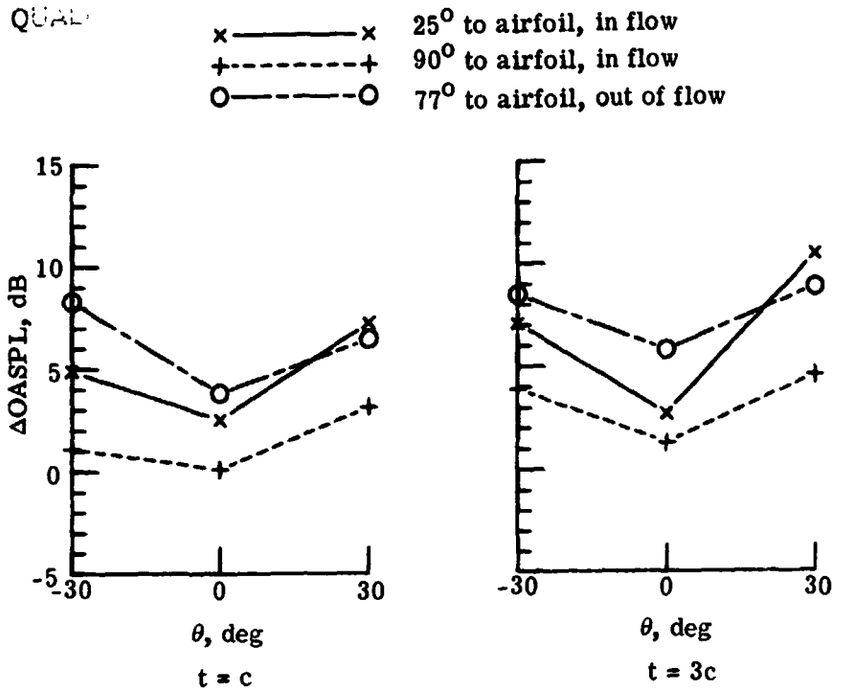

(a) Twin 1; $\beta_{.75}$ = 20°; T = 40 lb (178 N).

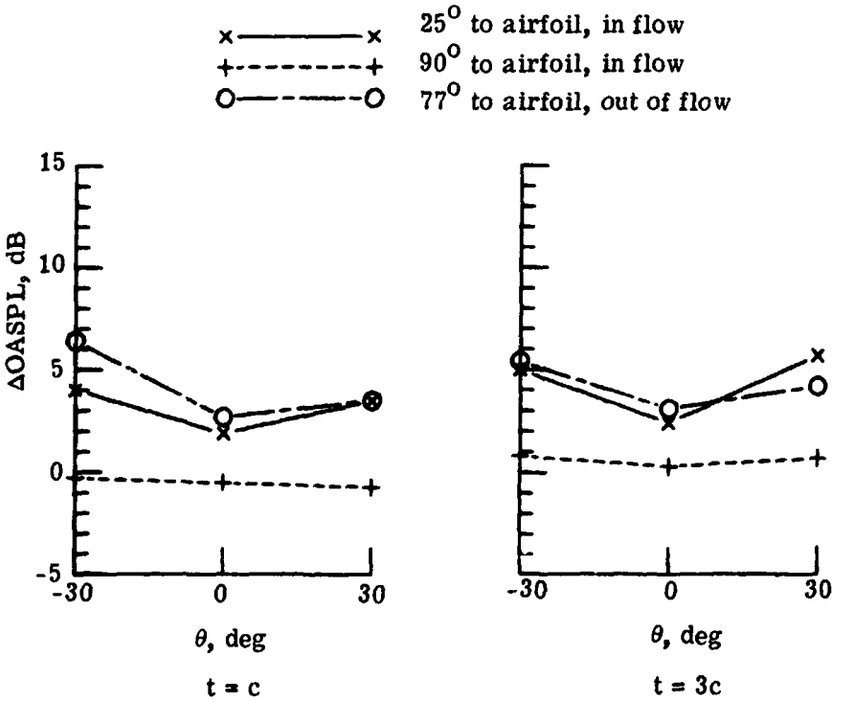

(b) Twin 1; $\beta_{.75}$ = 20°; T = 83 lb (369 N).

Figure 14.- Dependence of ΔOASPL on observer position with respect to disk plane.

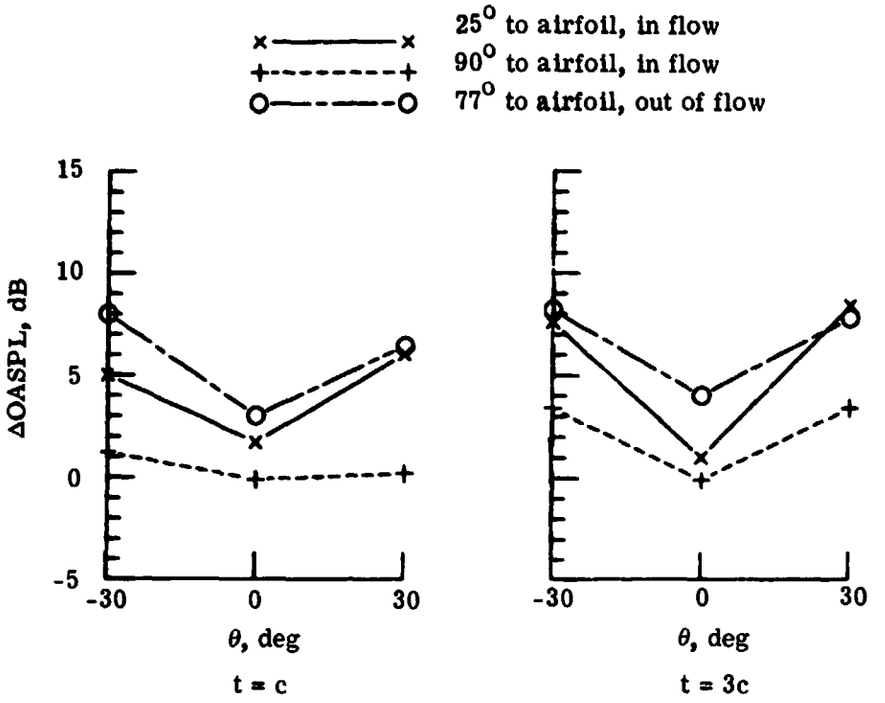

(c) Twin 3; $\beta_{.75}$ = 20°; T = 40 lb (178 N).

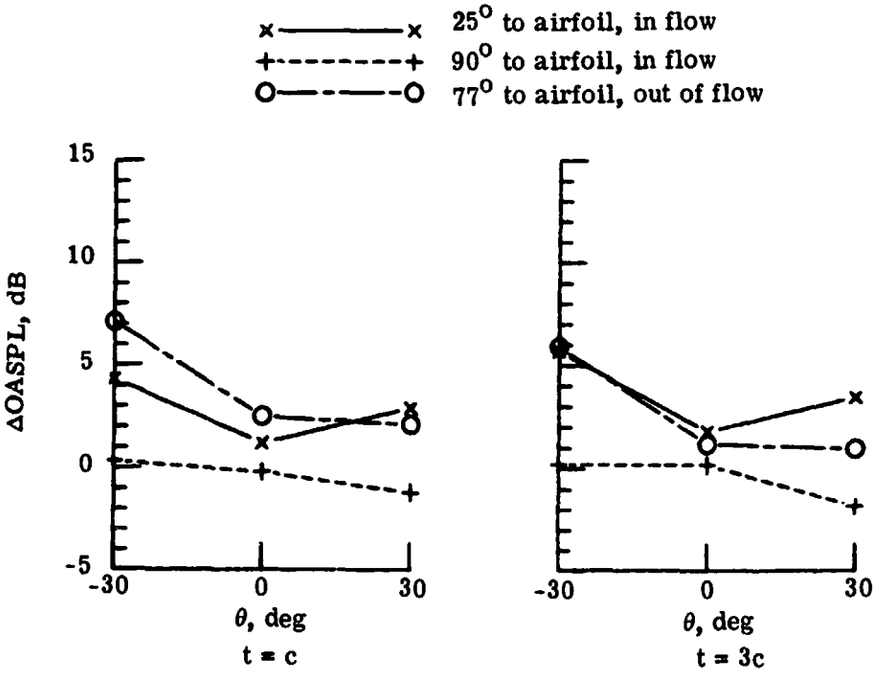

(d) Twin 3; $\beta_{.75}$ = 20°; T = 83 lb (369 N).

Figure 14.- Continued.

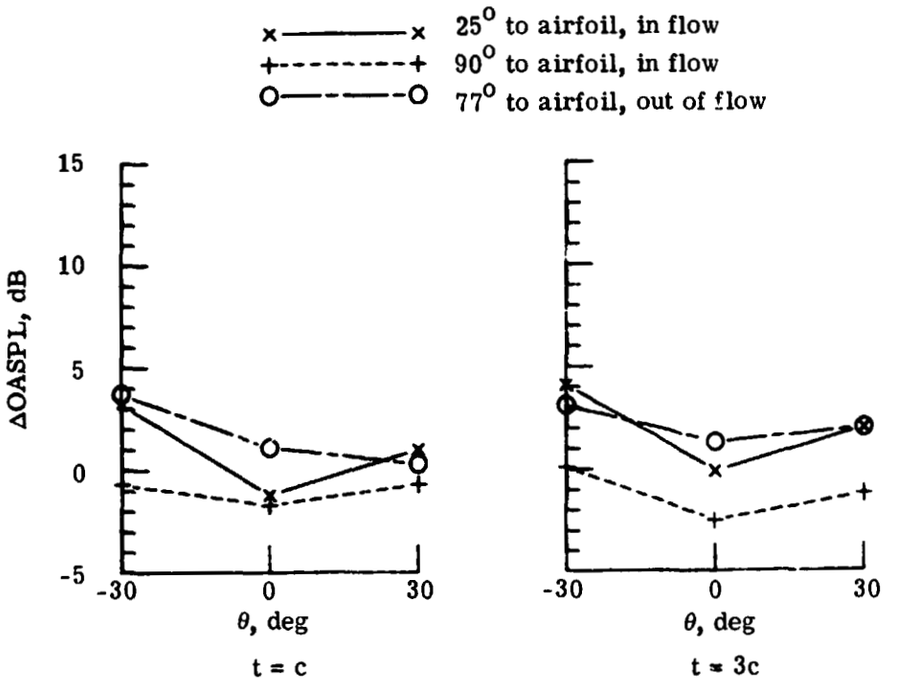

(e) Twin 3; $\beta_{.75}$ = 15°; T = 100 lb (445 N).

Figure 14.- Concluded.

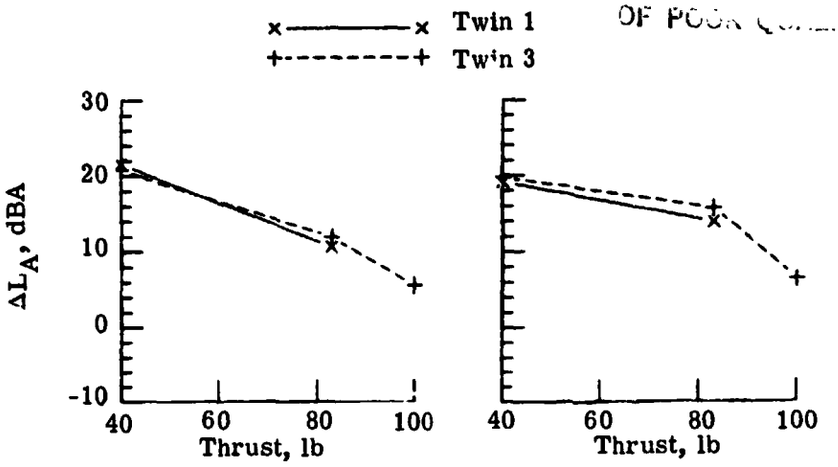

(a) Microphone 3a.

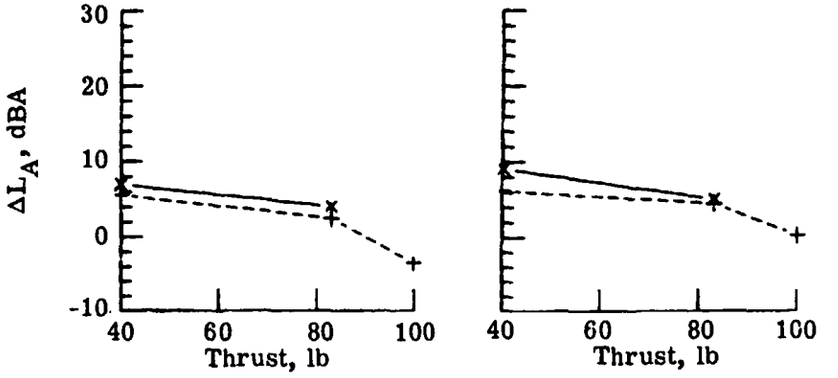

(b) Microphone 3b.

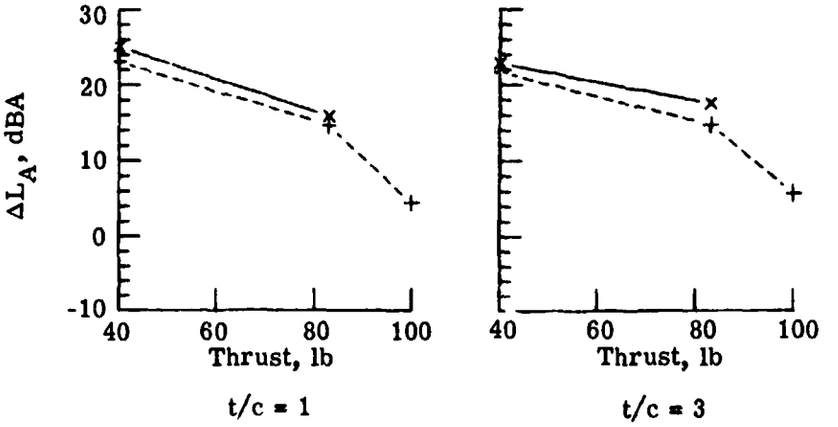

(c) Microphone 3c.

Figure 15.- Effect of propeller thrust on ΔL_A produced by propeller in wake. (1 lb = 4.45 N.)

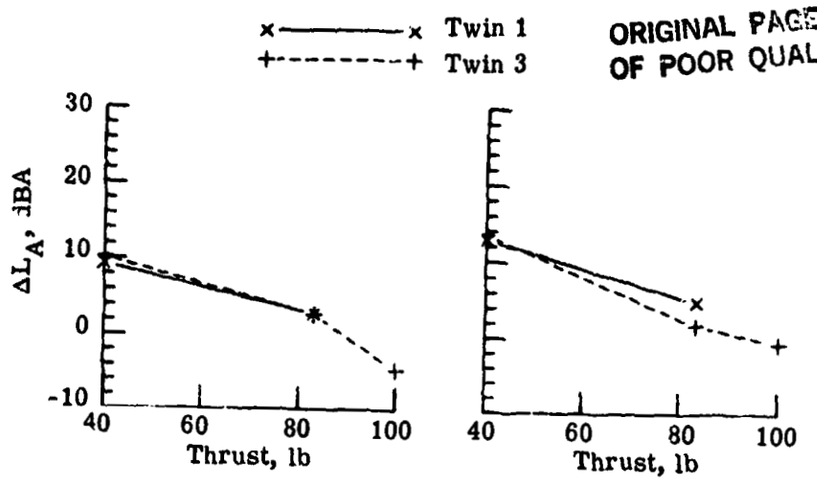

(d) Microphone 3d.

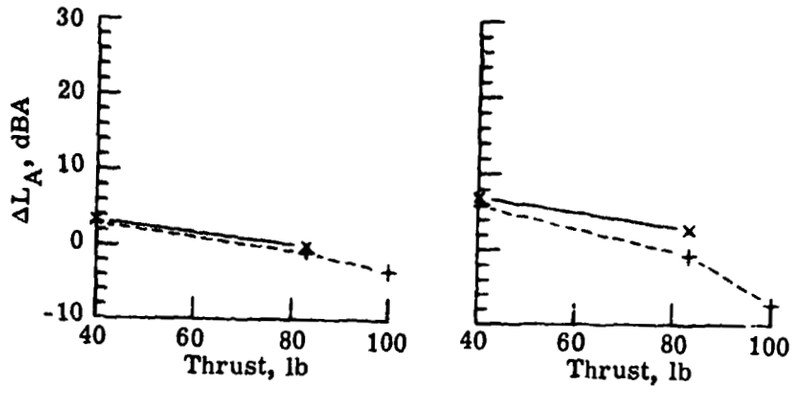

(e) Microphone 3e.

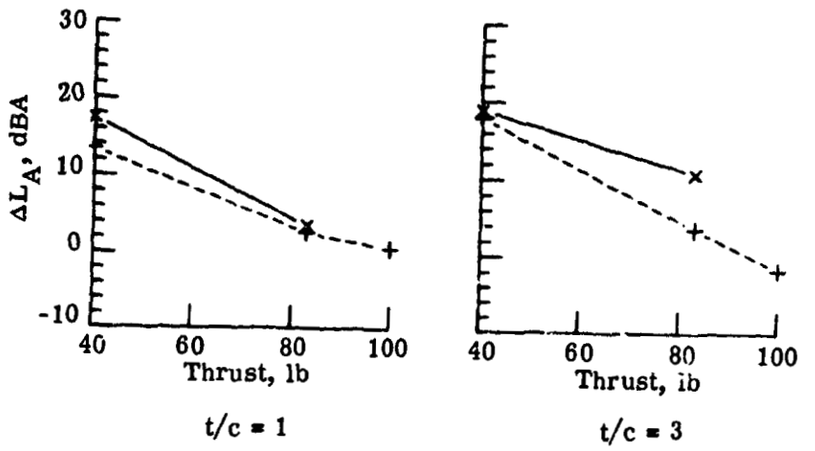

(f) Microphone 3f.

Figure 15.- Continued.

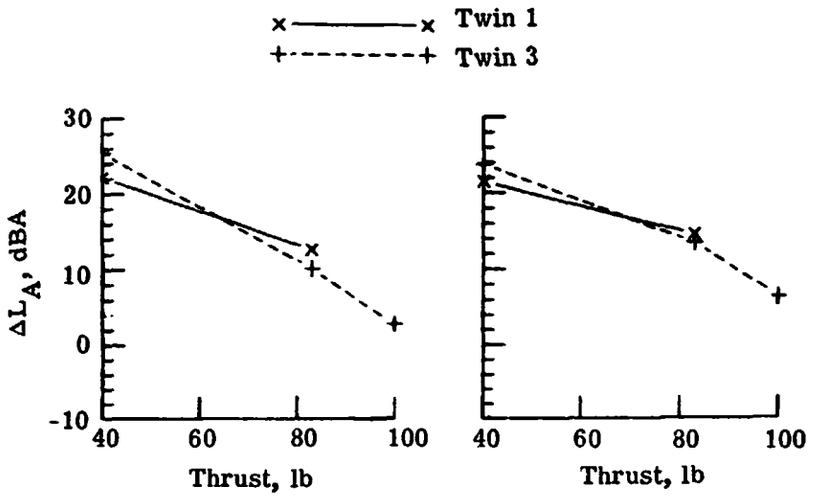

(g) Microphone 4.

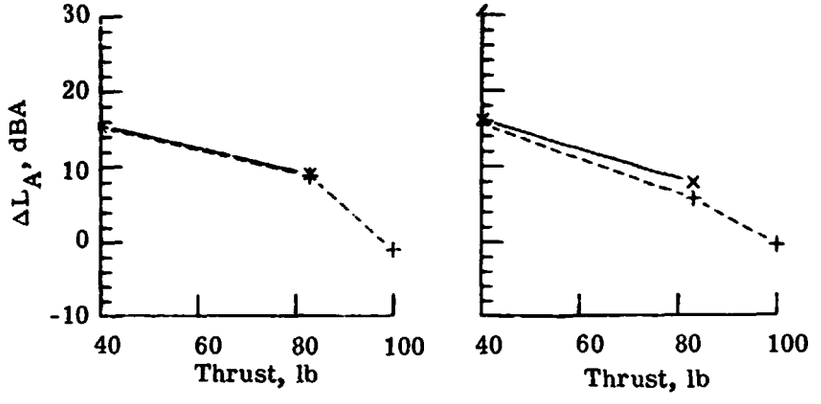

(h) Microphone 5.

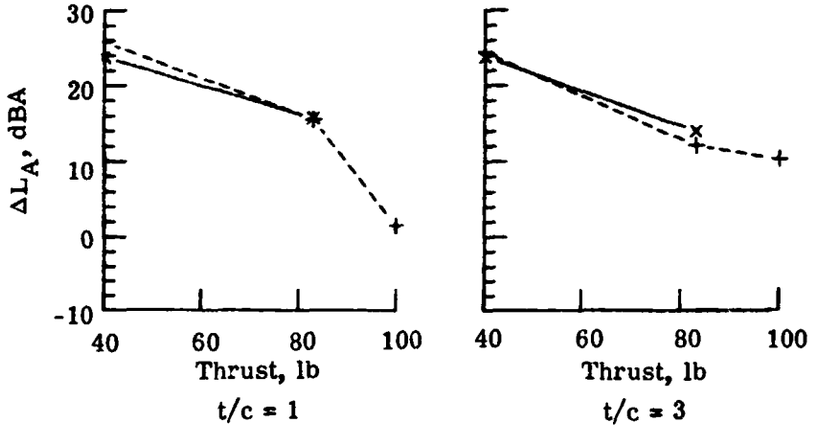

(i) Microphone 6.

Figure 15.- Concluded.

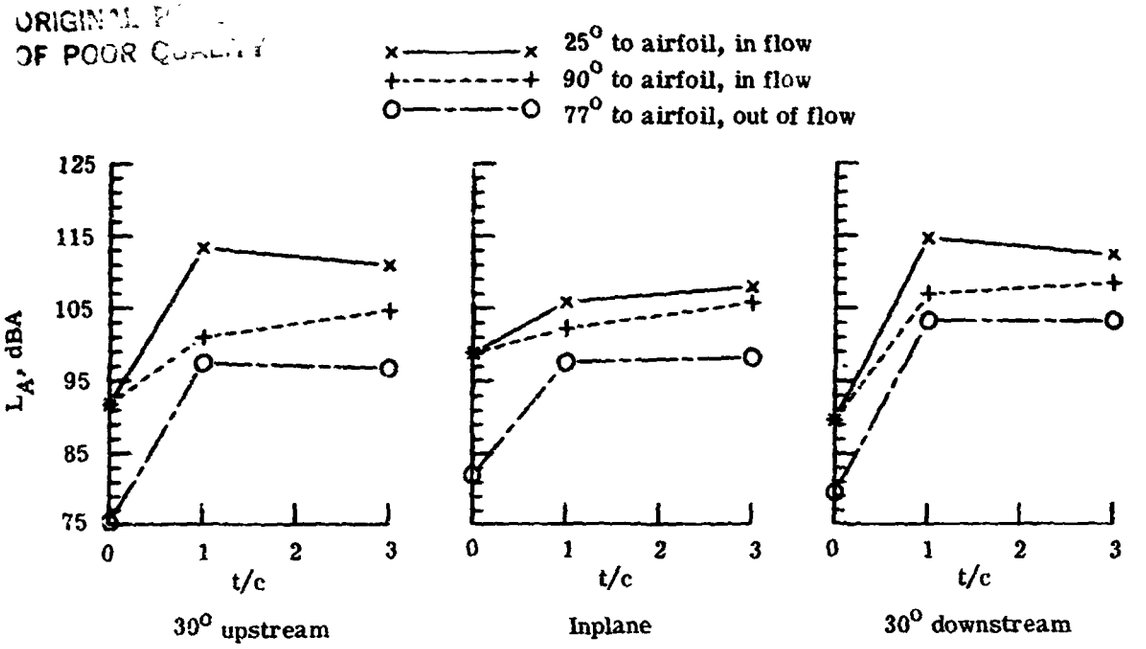

(a) Twin 1; $\beta_{.75}$ = 20°; T = 40 lb (178 N).

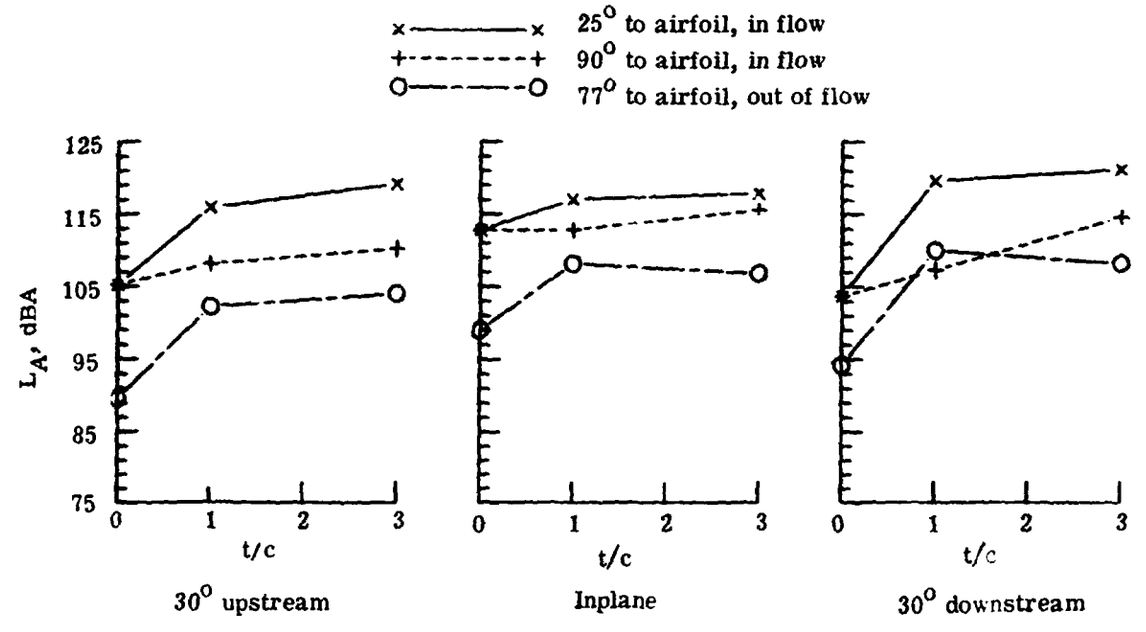

(b) Twin 1; $\beta_{.75}$ = 20°; T = 83 lb (369 N).

Figure 16.- Effect of wake thickness on L_A produced by propeller in wake.

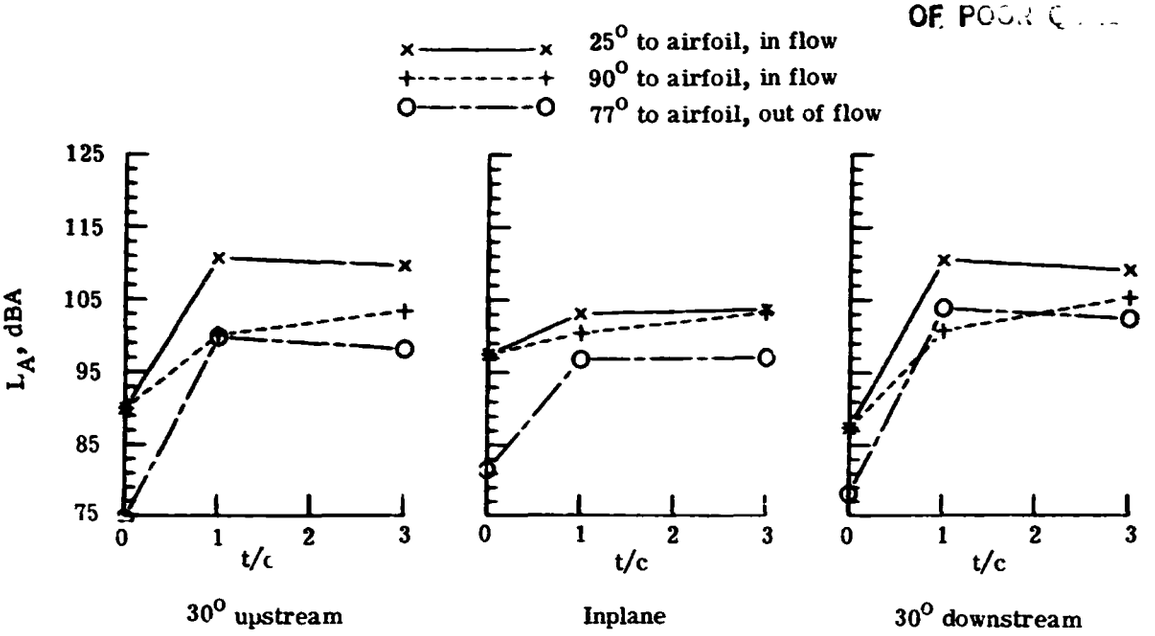

(c) Twin 3; $\beta_{.75}$ = 20°; T = 40 lb (178 N).

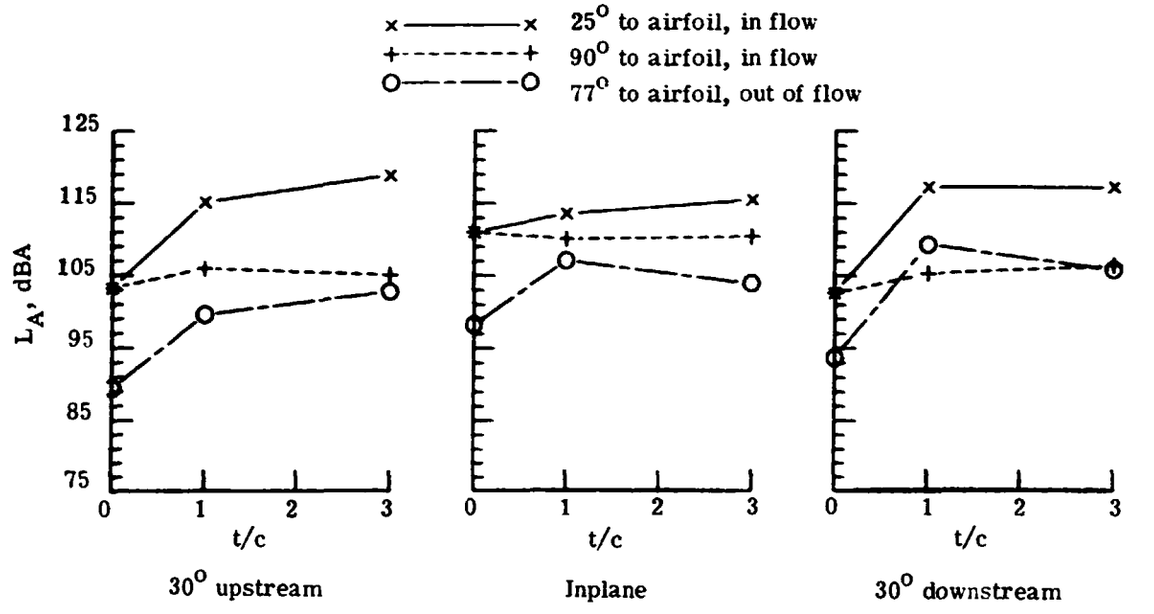

(d) Twin 3; $\beta_{.75}$ = 20°; T = 83 lb (369 N).

Figure 16.- Continued.

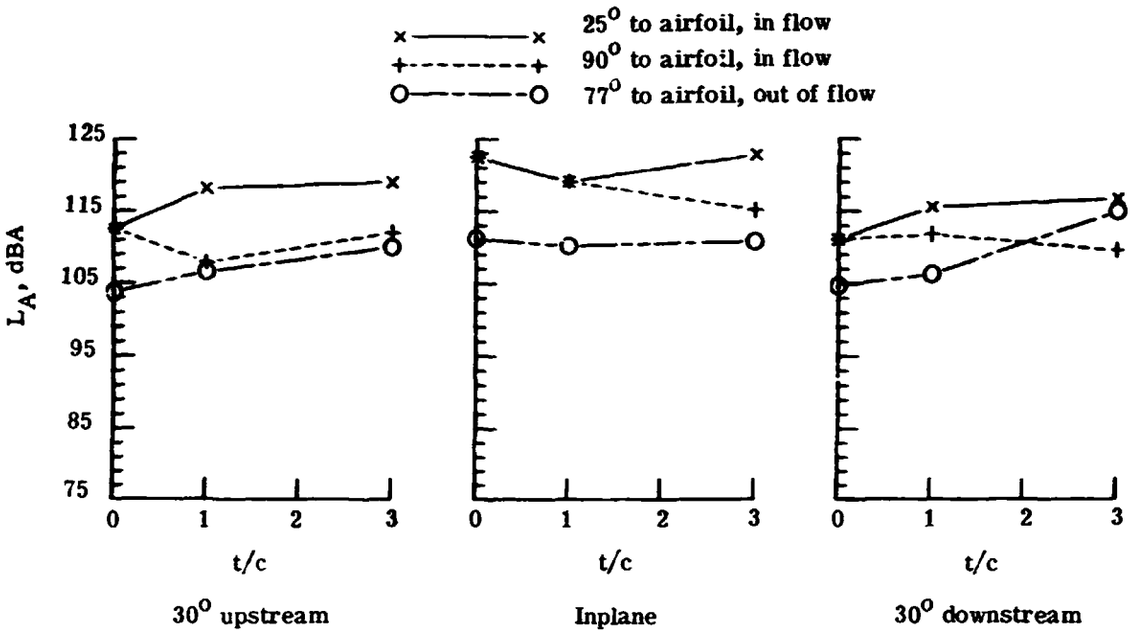

(e) Twin 3; $\beta_{.75}$ = 15°; T = 100 lb (445 N).

Figure 16.- Concluded.

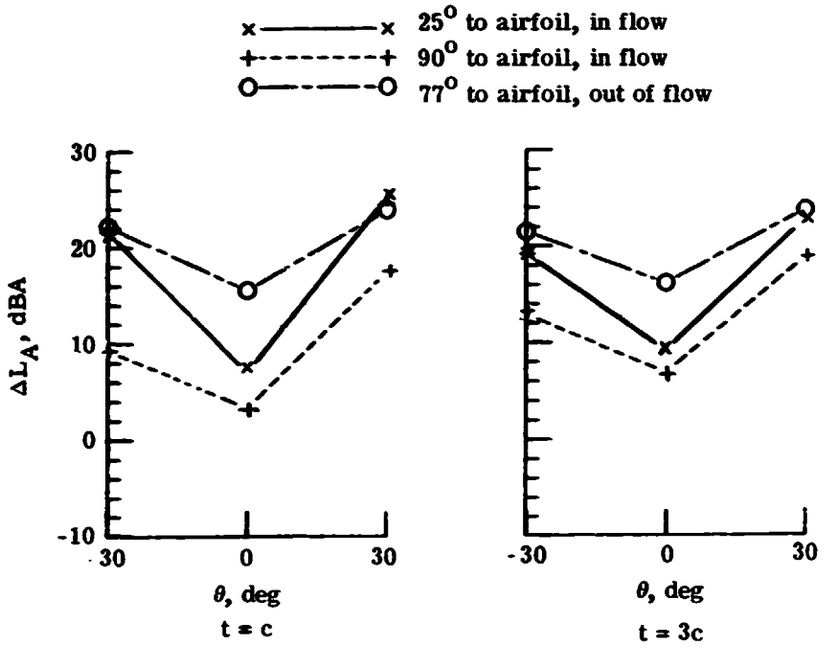

(a) Twin 1; $\beta_{.75}$ = 20°; T = 40 lb (178 N).

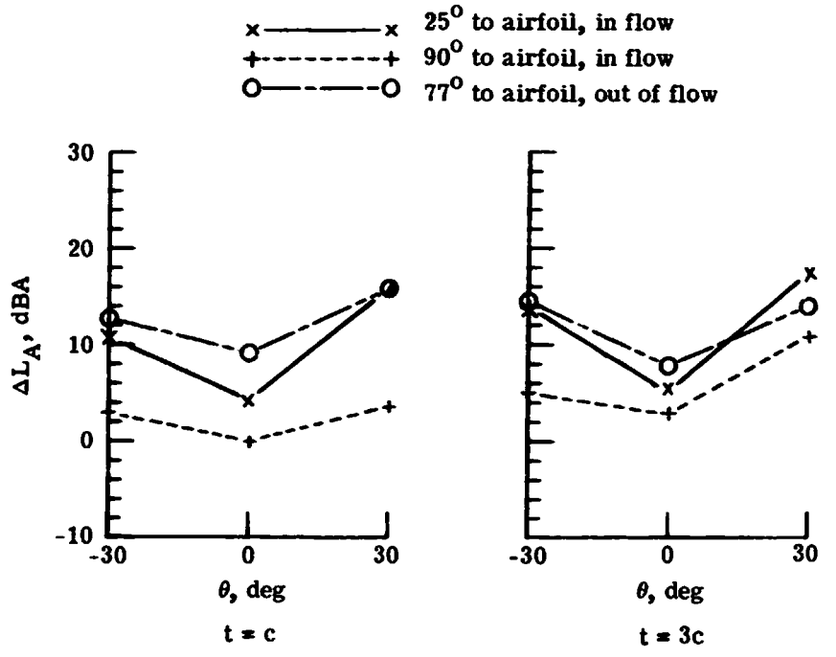

(b) Twin 1; $\beta_{.75}$ = 20°; T = 83 lb (369 N).

Figure 17.- Dependence of ΔL_A on observer position with respect to disk plane.

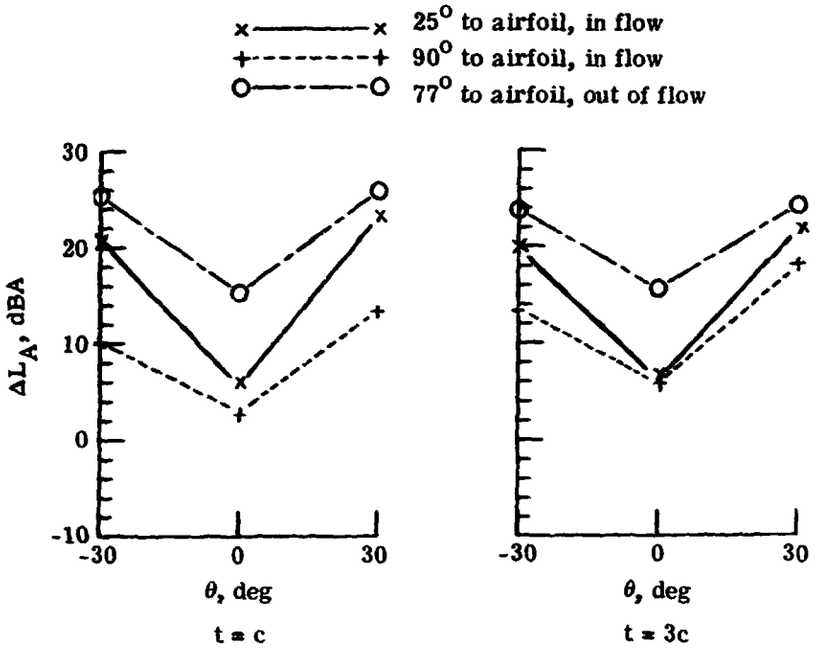

(c) Twin 3; $\beta_{.75}$ = 20°; T = 40 lb (178 N).

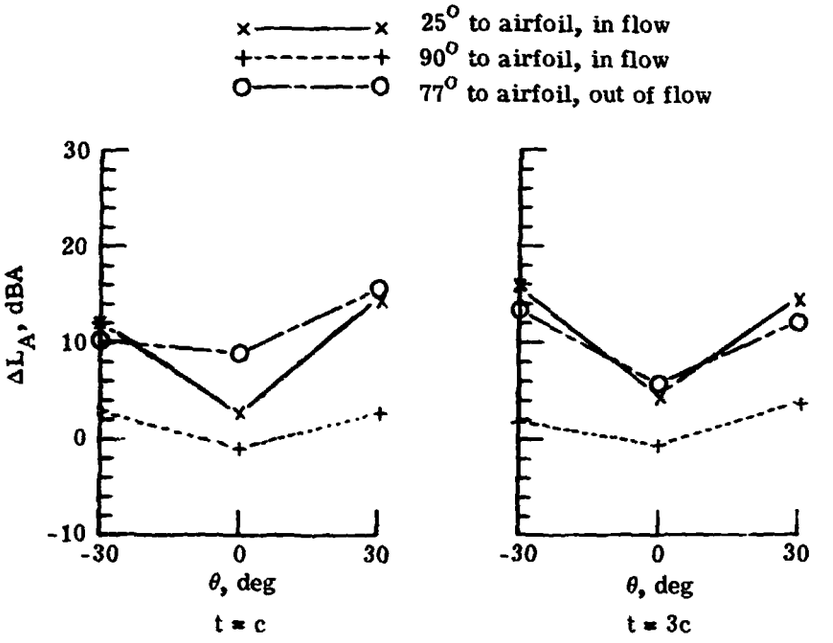

(d) Twin 3; $\beta_{.75}$ = 20°; T = 83 lb (369 N).

Figure 17.- Continued.

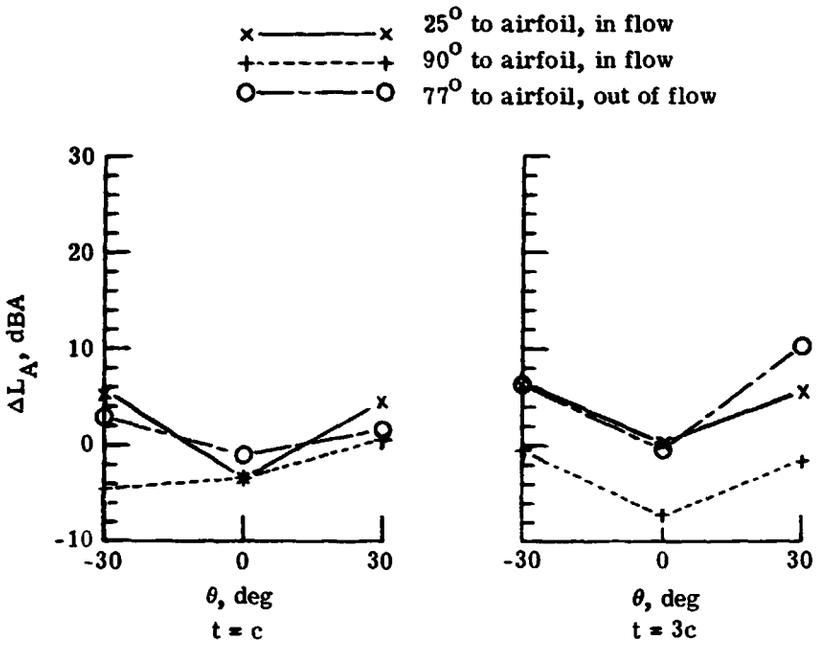

(e) Twin 3; $\beta_{.75}$ = 15°; T = 100 lb (445 N).

Figure 17.- Concluded.